CAPACITY AND THROUGHPUT OPTIMIZATION IN MULTI-CELL 3G WCDMA NETWORKS

Son Nguyen, B.S.

Thesis Prepared for the Degree of

MASTER OF SCIENCE

UNIVERSITY OF NORTH TEXAS

December 2005

APPROVED:

Robert Akl, Major Professor
Robert Brazile, Committee Member and Graduate Coordinator
Steve Tate, Committee Member
Krishna Kavi, Chair of the Department of Computer Sciences
Oscar N. Garcia, Dean of the College of Engineering
Sandra L. Terrell, Dean of the Robert B. Toulouse School of Graduate Studies

Nguyen, Son. *Capacity and Throughput Optimization in Multi-cell 3G WCDMA Networks*. Master of Science (Computer Science and Engineering), December 2005, 71 pp., 16 tables, 24 figures, references, 50 titles.

User modeling enables in the computation of the traffic density in a cellular network, which can be used to optimize the placement of base stations and radio network controllers as well as to analyze the performance of resource management algorithms towards meeting the final goal: the calculation and maximization of network capacity and throughput for different data rate services. An analytical model is presented for approximating the user distributions in multi-cell third generation wideband code division multiple access (WCDMA) networks using 2-dimensional Gaussian distributions by determining the means and the standard deviations of the distributions for every cell. This model allows for the calculation of the inter-cell interference and the reverse-link capacity of the network.

An analytical model for optimizing capacity in multi-cell WCDMA networks is presented. Capacity is optimized for different spreading factors and for perfect and imperfect power control. Numerical results show that the SIR threshold for the received signals is decreased by 0.5 to 1.5 dB due to the imperfect power control. The results also show that the determined parameters of the 2-dimensional Gaussian model match well with traditional methods for modeling user distribution.

A call admission control algorithm is designed that maximizes the throughput in multi-cell WCDMA networks. Numerical results are presented for different spreading factors and for several mobility scenarios. Our methods of optimizing capacity and throughput are computationally efficient, accurate, and can be implemented in large WCDMA networks.

ACKNOWLEDGMENTS

First and foremost, I would like to give my heartfelt thanks to my advisor Dr. Robert Akl for taking on multitude of roles that provided guidance and direction. During this journey, I had sometimes felt I could not progress any further, but his whole-hearted devotion and enthusiasm not only kept me on track but also lightened up the way to the completion of this work. Furthermore, I am highly indebted to the members of my committee Dr. Robert Brazile and Dr. Steve Tate for their careful reading and suggestions.

I am also very grateful to my parents for their unconditional love and many years of support. Above all, I would like to thank Khanh Ha Nguyen who has been an inspiration and a partner from the very beginning.

CONTENTS

LIST OF TABLES

LIST OF FIGURES

CHAPTER 1

INTRODUCTION

1.1 CDMA History

The global mobile communications market has expanded very rapidly [13]. From analog phone systems in the 70's and 80's, cellular phone systems have progressed to digital cellular systems in their second generation (2G) with Time Division Multiple Access (TDMA), Frequency Division Multiple Access (FDMA), and Code Division Multiple Access (CDMA) technologies in the 90's. Society has seen the introduction of data services from 2.5G with Short Message Service and now new third generation (3G) mobile phone systems are being introduced where cellular phones can access Internet services, retrieving text, pictures, video and other documents, with a promised delivery speed of up to 2 Mbps.

Almost 1.52 billion people were using mobile phones by the end of 2004, and according to the new study by the Yankee Group, this number could reach 1.87 billion (27.4% total world population) by the end of 2007 [30]. CDMA has been the fastest-growing digital wireless technology since its first commercialization in 1994. 240 million subscribers already existed worldwide by the end of 2004 [15]. The major markets for CDMA are North America, Latin America, and Asia (particularly Japan and Korea). In total, CDMA was adopted by more than 100 operators across 76 countries around the globe [16]. According to [25, 50], CDMA technology can offer about 7 to 10 times the capacity of analog technologies and up to 6 times the capacity of digital technologies such as TDMA. The advantages over TDMA and FDMA technologies, such as voice quality, system reliability, and handset battery life, have created a numerous of research on CDMA systems.

1.2 Objectives

In this work, the 2-dimensional (2-D) Gaussian function is used to model user distribution in cellular networks. In addition, capacity in Wideband Code Division Multiple Access (WCDMA) cellular networks is calculated and optimized for different data rate services.

The objectives of this work are as follows:

- **User distribution modeling with 2-D Gaussian function:**
  - Modeling user distribution by determining the user densities, the means, and the standard deviations of the 2-D Gaussian function in every cell.
- **WCDMA capacity:**
  - Formulation and calculation of the maximum capacity for different services in WCDMA networks based on given quality of service (QoS) constraints.
- **WCDMA call admission control and throughput:**
  - Formulation and calculation of Call Admission Control (CAC) in WCDMA networks based on the QoS and Grade of Service (GoS) constraints. This leads to the maximization of the throughput in WCDMA networks.

1.3 Organization

In Chapter 2, CDMA and WCDMA technologies are introduced. While CDMA is a 2G cellular system with a main focus on voice services, WCDMA is the emerging technology for 3G mobile phone systems with different data rates on demand for serving different services for users. This chapter summarizes features as well as key points, which demonstrate CDMA's superiority over other 2G cellular networks. These superior features include power control, user activity detection, soft handoff, and cell sectoring. In addition, this chapter

also introduces the requirements for 3G cellular systems, which include wider bandwidth allocations, as well as new additional features of 3G WCDMA cellular networks.

In Chapter 3, the 2-D Gaussian function is used in modeling users in cellular networks. This method when used to calculate the average interference can more rapidly and efficiently compute the capacity in WCDMA networks when compared to other methods, like actual interference, which are computationally intensive.

In Chapter 4, the formulation and calculation of the maximum capacity in WCDMA cellular networks is described. Our optimization with given quality of service constraints can find the maximum number of simultaneous users for voice and data services in 3G networks.

In Chapter 5, a call admission control algorithm is designed that maximizes the throughput in multi-cell WCDMA networks. Numerical results are presented for different spreading factors and for several mobility scenarios.

Finally, in Chapter 6, the conclusions are presented, which summarize the contributions of this work.

CHAPTER 2

CDMA AND WCDMA OVERVIEW

2.1 Introduction to CDMA

Code Division Multiple Access (CDMA) is a fairly new wireless communication technology, which was introduced by Qualcomm in the early 90's. Compared to existing technologies such as FDMA and TDMA, which use different frequency sub-bands and time slots respectively, to carry multiple calls, CDMA distinguishes different calls by unique codes, which are assigned individually to each call. Fig. 2.1 depicts the differences between the three technologies.

CDMA has many advantages over TDMA and FDMA technologies in cellular networks. These advantages include increased capacity, immunity to multi-path fading, voice activity, and soft handoff mechanism. These gains and features yield better longevity of CDMA handset battery life and higher quality of voice signals. According to [25], an analysis made by the Telecommunications Research and Action Center found CDMA outperformed other digital and analog technologies on every front, including signal quality, security, power consumption, and reliability.

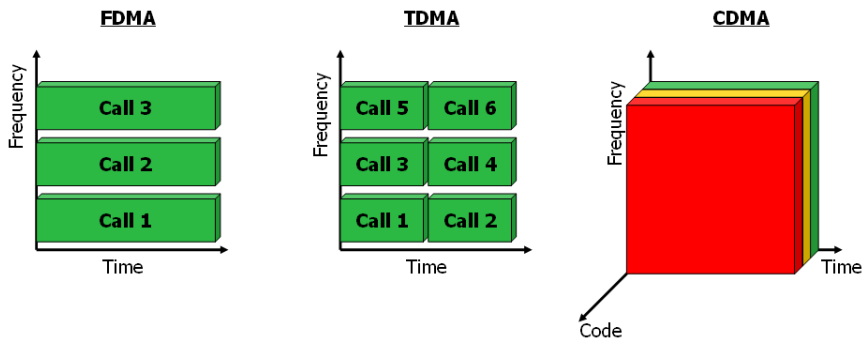

Figure 2.1: Comparison between FDMA, TDMA, and CDMA.

CDMA is based on Spread Spectrum (SS) communication, a technique which was developed during World War II. The essential idea behind SS is spreading the information signal over a wider bandwidth to make jamming and interception more difficult. There are three types of SS: Frequency Hopping, Time Hopping, and Direct Sequence (DS). The first type of spread spectrum is known as Frequency Hopping in which the signal is broadcasted over a seemingly random series of radio frequencies, hopping from frequency to frequency at a fixed interval, as shown in Fig. 2.2. By knowing the hopping sequence, which is contained in the spreading code, the receiver, hopping between frequencies in synchronization with the transmitter, picks up the message. Time Hopping is the second type of SS where the transmission time is divided into equal amounts of time intervals called frames. Each frame is divided into time slots. During each frame, only one time slot is used to transmit the message, as shown in Fig. 2.3. Time Hopped systems assume that the sender and the receiver know the length of each time frame and the sequence of time slots in which the message will be modulated. The third spreading technique is Direct Sequence. Direct Sequence Spread Spectrum modulates the data with a fast pseudo-random code sequence. With DS, each bit in the original signal is modulated to multiple bits in the transmitted signal by using the spreading code. With the spreading code, the signal is spread across a wider frequency band in direct proportion to the number of bits used. At this time, DS is the prefered spreading technique in CDMA and WCDMA and thus is the only one considered in this work.

With DS-CDMA, each user's signal is modulated with a high-rate special code (pseudo-random binary sequence), which is assigned by the Base Station (BS), into a wideband signal transmitted over the air medium. CDMA users share the same frequency spectrum; thus, CDMA signals appear to overlap in the time and frequency domain as was shown in Fig. 2.1. Each user's signal is distinguished by its special code. The only way to despread the signal to recover the message for a user is to use each user's own special code. Only the subscribed BS knows all its users' special codes. For each individual user, other signals from

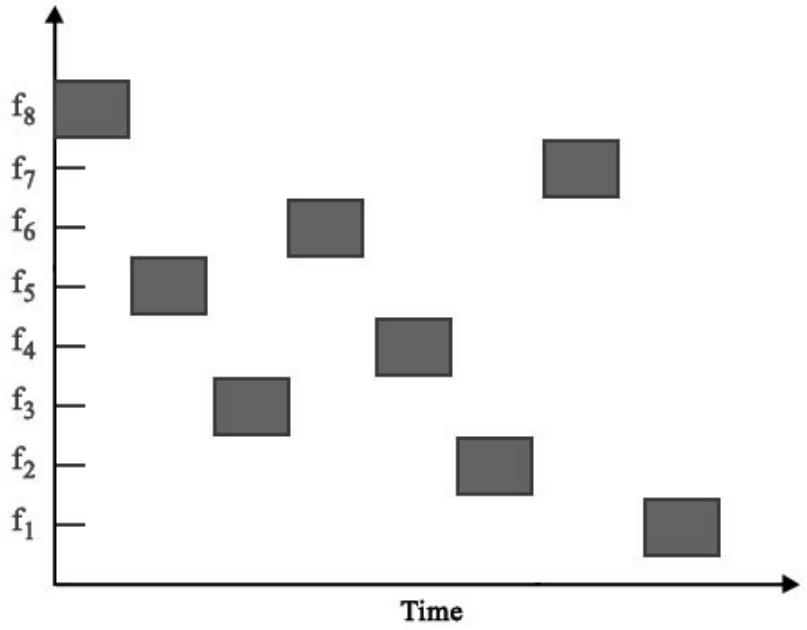

Figure 2.2: Frequency Hopping Spreading Spectrum.

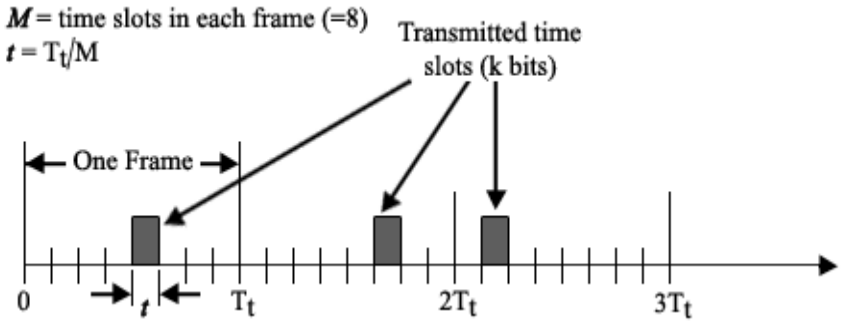

Figure 2.3: Time Hopping Spreading Spectrum.

different users appear as noise and are represented as interference generated by the system. In a CDMA network, the signal for each user is required to be above a given signal-to-interference ratio (SIR) threshold for it to be received and despread by the BS correctly. Therefore, the capacity of a CDMA network is limited by the amount of interference that is generated by all users in the network (unlike FDMA and TDMA capacities, which are fixed and primarily bandwidth limited).

2.1.1 Power Control

Since the capacity of a CDMA network is interference-bound, the study of capacity characteristics focuses primarily on the methods of reducing interference. Fast and precise power control is a key requirement for CDMA technology. Power control aims to reduce interference by minimizing the effects of the near-far problem (the received power at a BS from a mobile station (MS) near the cell boundary is less compared to a MS close to the BS), co-channel interference, and fading while keeping the received signal power, or the SIR, at the same level at the BS. In addition, power consumption can be significantly reduced in the MS, which results in increasing longevity of the MS. Research on power control algorithms [19, 23, 27, 28, 52, 61, 77] has substantially investigated the near-far problem. In [54], the authors propose an adaptive SIR based feedback power control, which tries to solve the near-far problem while maintaining a low co-interference effect by individually adjusting the SIR threshold control level for each mobile station, with respect to its own radio link. This control level is established by using Fuzzy Logic Control. In [8], the authors investigate a feedback power control approach that allows power commands to be updated at a faster rate compared to the rate of multipath fading. In [73, 76] the authors define the problem of SIR balancing to be an eigenvalue problem in a link-gain matrix, and try to find the optimum downlink power control.

There are two main different methods for managing power control: open-loop and closed-

loop. Open-loop power control determines the transmit power such that the sum of transmit power and the received power is kept constant. Closed-loop power control involves with two parties - BS and MS, in which one party signifies the other party to increase or decrease its transmit power by a *power step* such that the target received $\frac{E_b}{I_o}$ achieves a given threshold.

2.1.2 Frequency Reuse

In TDMA and FDMA, the total bandwidth is divided into a number of channels. Each user is assigned a channel for an uplink (the frequency that a MS sends information to a BS) and a downlink (the frequency that a BS transmits the signal to a MS). The transmitted signal is attenuated with both fast (Rayleigh) and slow fading. Thus, with precise power control, different cells in a cellular network can use the same frequencies if the signals from the same frequencies from one cell will not reach the BS of another cell. This concept is called frequency reuse capability. In a hexagonal cellular network structure, the frequency reuse factor may be 4, 7, or 12. Because a cellular network is given a pre-determined range of frequencies to exchange information between the BSs and MSs, if the frequency reuse factor, which the cellular network can employ, is smaller, then the network can obtain a higher capacity. CDMA cellular systems typically use universal frequency reuse (or a frequency reuse factor of 1), where the MSs and BSs use the whole bandwidth to transfer and receive information.

2.1.3 Voice Activity Detection

In CDMA systems, reducing multiple access interference from neighboring cells results in a capacity gain. Since CDMA systems use speech coding, reducing the rate of the speech coder with voice activity detection along with variable rate data transmission could decrease the multiple access interference. According to [33], the voice activity factor for human speech averages about 42%. In [24, 33], the authors show that increasing the voice activity factor or

data activity factor could reduce the network capacity significantly. In FDMA and TDMA cellular systems, the frequencies are permanently assigned to users and BSs as long as there is a communication between them. Thus, the capacity in FDMA and TDMA systems is fixed regardless whether the systems employ voice or data activity detection.

2.1.4 Cell Sectoring

Due to increasing demand for cellular communication without corresponding increases in bandwidth allocation, the authors in [11, 12, 57] introduce Cell Sectoring (Spatial Processing) to improve spectrum utilization. Cell Sectoring is a method that uses multiple directional antenna arrays to reduce the co-channel interference, resulting in increased cellular network capacity. According to [42, 56], resolving angular positions of the mobiles by using antenna arrays at BSs, both in receiving and transmitting, can lead to many-fold increases in system capacity.

2.1.5 Soft Handoff

Soft handoff (handover) is one of the most attractive features of CDMA technology. Soft handoff is a technique that allows a MS in transition between two or more adjacent cells to transmit and receive the same signal from these BSs simultaneously. By employing universal frequency reuse and a Rake receiver (see [58] pages 49-56), each individual MS can isolate and align both in time and in phase to reinforce the forward signals from different BSs, as well as to transmit its signal to all the BSs. On the uplink side, the Mobile Switching Center must first combine and resolve the signals from all the BSs and then determine which BS is receiving the stronger and better replica. Depending on the relative received signal strength, decisions are made as to when to enter soft handoff and when to release the weaker BS. Recent improvements in soft handoff algorithms are described in [9, 75]. Experimental data in [70] have shown that using soft handoff increases cell coverage resulting in increased capacity

in CDMA networks. In [17], a comparison between hard handoff (in TDMA/FDMA) and soft handoff (in CDMA) shows that under a variety of conditions, the shadow fading margin required by CDMA soft handoff is less than TDMA/FDMA systems by 2.6-3.6 dB, which translates to range extension for CDMA cellular networks. In [35], the authors compare the network capacity gain with different parameter sets for new soft handoff algorithm in IS-95A [64] and IS-95B [63]. Soft handoff, however, requires complex design and implementation. Recent surveys [39, 74] of soft handoff show what technical issues need to be resolved. In addition, the surveys show what the benefits and tradeoffs of using soft handoff and discuss feasible parameter settings.

Extensive research has been done on calculating the reverse link capacity of single and multi-cell CDMA networks [10, 20, 31, 46, 51, 53, 59, 60, 71, 72]. These studies conclude that the capacity of the reverse link is lower than the capacity of the forward link. In [26], the authors analyze both reverse link and forward link capacity under the assumption of ideal power control and hard handoff circumstances. The reverse link capacity limits the system capacity; however, only a small difference exists between forward and reverse link capacity. In this work, only the reverse link capacity is considered.

Most of the models [7, 38, 40, 62] use average inter-cell interference instead of actual inter-cell interference for capacity analysis. In an average inter-cell interference model, the interference caused by different users in the same cell is identical, and is independent of their exact location within a cell. Thus, accurate user modeling becomes essential for average interference calculation. In this work, average inter-cell interference is used to model and calculate capacity in WCDMA cellular networks.

2.2 WCDMA Overview

Third generation (3G) systems are designed for multimedia communication, which includes person-to-person communication with high-quality images and video and high rate accessing

of information and services on public and private networks, up to 2 Mbps. These new systems will create new business opportunities, not only for the cellphone, infrastructure, and hardware manufactures and their operators, but also for the applications and content providers carried by these networks (i.e., paid video games, music, video, and ring tones downloading).

WCDMA specifications have been created in 3GPP (3rd Generation Partnership Project), which is the joint standardization project of the bodies from Europe, Japan, Korea, the US, and China. Within 3GPP, WCDMA is identified as UTRA (Universal Terrestrial Radio Access) FDD (Frequency Division Duplex) and TDD (Time Division Duplex). The name WCDMA is used to cover both FDD and TDD operations.

The process of developing third generation mobile systems started in a 1992 meeting of the World Administrative Radio Conference (WARC), which is under the International Telecommunication Union (ITU). In the meeting, the frequencies around 2 GHz were identified to be available in most countries to be used by the future third generation mobile systems, both uplink and downlink as shown in Fig. 2.4 [29]. Under the ITU, these third generation systems are called International Mobile Telephony 2000 (IMT-2000).

There are three major air interfaces proposed for 3G cellular systems: Enhanced Data Rate for GSM Evolution (EDGE), W-CDMA, and CDMA2000 [34]. The spectrum allocation for IMT-2000 (or WARC-92) bands of 2x60MHz (1920-1980 MHz plus 2110-2170 MHz) are available in Europe, Japan, Korea, and most Asian countries. The two spectrums for IMT-2000 TDD bands (1900-1920 MHz and 2020-2025 MHz) are available in Europe and Korea. In Japan, part of the IMT-2000 spectrum TDD is used by cordless telephone systems. In the United States, at the time of the 1992 meeting, no new spectrum had yet been made available for third generation systems. In the United States, third generation services can be implemented using the existing PCS spectrum with alternative technologies, including EDGE, WCDMA, and CDMA2000.

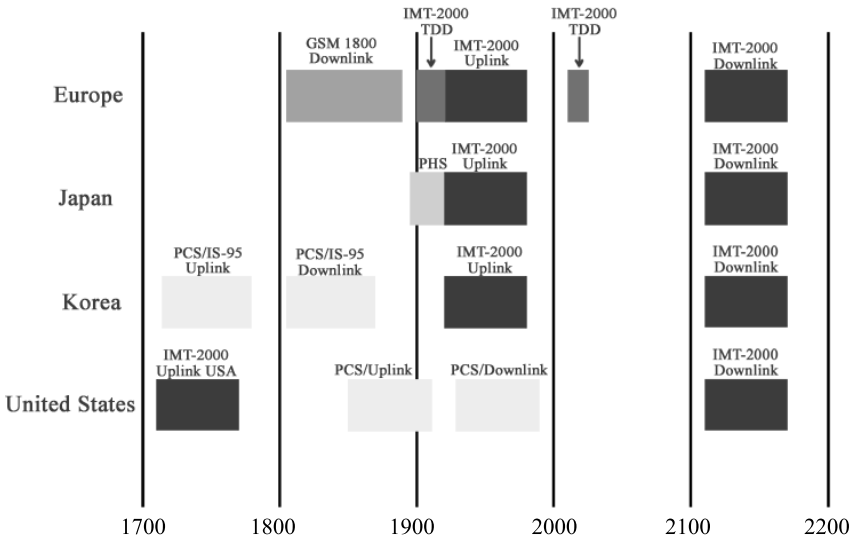

Figure 2.4: 2 GHz band spectrum allocation in Europe, Japan, Korea, and US (MSS = Mobile Satellite Spectrum).

At the ITU-R WRC-2000 in May 2000, the following additional frequency bands were also introduced for IMT-2000: 1710-1885 MHz, 2500-2690 MHz, and 806-960 MHz

According to [29], new third generation spectrums in the United States are expected to have 2x60 MHz (1710-1770 MHz and 2110-2170 MHz) assigned. These two spectrums can be efficiently used to carry 3rd generation services with WCDMA. The new IMT-2000 spectrum 190 MHz (2500-2690 MHz) arrangement is still under discussion.

In the past, 2G cellular mobile phone systems mainly concentrated on voice traffic; now, 3G systems face the challenge of making data services wireless. In addition, the following characteristics are the new requirements of 3G systems:

- Data communication speeds up to 2 Mbps.
- Meet delay requirement constraints for different real-time services, including delay-sensitive real-time traffic (stock information) to best-effort packet data (video or voice).
- Variable bit data rates on demand.

Table 2.1: Main differences between WCDMA and IS-95 air interfaces. *WCDMA for UMTS: Radio Access for Third Generation Mobile Communication.* H. Holma and A. Toskala, 2002. Copyright John Wiley & Sons Limited. Reproduced with permission.

	WCDMA	IS-95
Carrier Spacing	5 MHz	1.25 MHz
Chip rate	3.84 Mcps	1.2288 Mcps
Power control frequency	1500 Hz, both uplink and downlink	Uplink: 800 Hz, downlink: slow power control
Base station synchronization	Not needed	Yes, typically obtained via GPS
Inter-frequency handovers	Yes, measurements with slotted mode	Possible, but measurement method not specified
Efficient radio resource management algorithms	Yes, provides required quality of service	Not needed for speech only networks
Packet data	Load-based packet scheduling	Packet data transmitted as short circuit switched calls
Downlink transmit diversity	Supported for improving downlink capacity	Not supported by the standard

- Mix of services with different quality requirements on a single connection, including voice, video, and packet data.
- Quality of service (QoS) requirements from 10^{-6} bit error rate to 10% frame error rate.
- Coexistence with second generation systems and feasible solutions for inter-system handovers, which include coverage enhancements and load balancing.
- Higher spectrum efficiency.
- Support asymmetric uplink and downlink traffic, e.g., web browsing results in more downlink than uplink traffic.
- Coexistence of FDD and TDD modes.

The main differences between WCDMA and IS-95 are shown in Table 2.1 [29]. IS-95

is a second generation cellular network, which operates on the same frequency band as the Advanced Mobile Phone System (first generation cellular network), using FDD with a total bandwidth of 25 MHz in each direction [25]. Both WCDMA and IS-95 use direct sequence CDMA. WCDMA uses a higher chip rate of 3.84 Mcps. According to [29], the higher chip rate in WCDMA enables higher bit rates while providing more multipath diversity, which improves the coverage of a network when cellular equipments are employed with Rake receivers [17].

WCDMA uses fast closed-loop power control in both uplink and downlink, while IS-95 uses fast power control only in the uplink. The inclusion of fast power control at the MS side improves link performance and increases downlink capacity. However, it increases the complexity in the design of the MS.

The IS-95 system was designed to target mainly macro cellular applications. The macro cell BSs are required to be located on masts or rooftops where GPS signals can be easily received. IS-95 BSs are required to be synchronized and this can be done through the GPS system [47]. Since GPS reception is difficult without line-of-sight connection to the GPS satellites, the deployment of indoor and micro cells was a challenge until recent technology, indirect GPS, was developed [47]. BSs in WCDMA are designed to operate under asynchronous mode; thus, no synchronization from GPS is needed.

WCDMA changed the way communication is done in the core networks as shown in Fig. 2.5 [29]. In 2G and 2.5G CDMA cellular systems, all services (voice, SMS, WAP, and email) were using circuit switched core networks. In March 2000, 3GPP Release '99 kept voice and video services under circuit switched, while transforming SMS, WAP, and email to packet switched core networks. Also, Web, MMS, and Streaming services were added to packet switched core networks. The latest releases 5 and 6 of 3GPP have made all services use packet switched core networks [1, 29]. These releases have led to WCDMA implementations to work with asynchronous BSs, where no synchronization from GPS is necessary. The

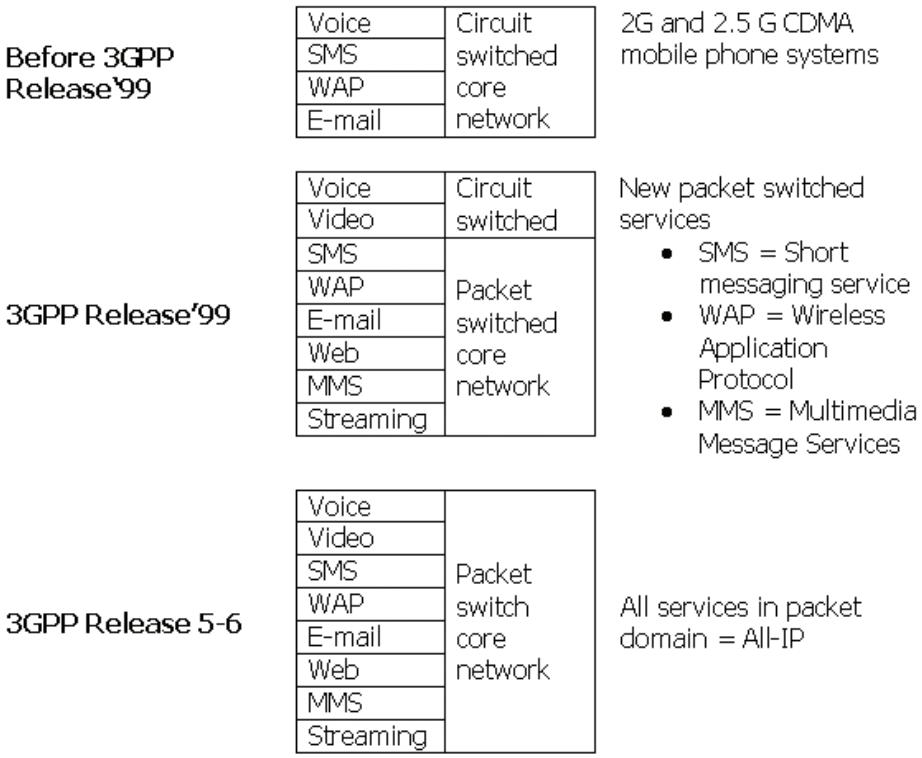

Figure 2.5: Development to all-IP for 3G services. *WCDMA for UMTS: Radio Access for Third Generation Mobile Communication*. H. Holma and A. Toskala, 2002. Copyright John Wiley & Sons Limited. Reproduced with permission.

asynchronous BSs have made the handoff in WCDMA different from IS-95.

Inter-frequency handoff is essential in WCDMA to maximize the use of several carriers per BS, while in IS-95 inter-frequency measurements are not specified.

CHAPTER 3

USER AND INTERFERENCE MODELING USING 2-D GAUSSIAN FUNCTION

3.1 Introduction

Radio Network Planning is the problem of dimensioning, which is a process of finding possible configurations and the amount of network equipment needed for an operator's coverage, capacity, quality of service, area type, and radio propagation requirements. Specifically, dimensioning activities involve radio link budget and coverage analysis, capacity calculation, and an estimation on the amount of sites, base station hardware, radio network controllers, equipments at different interfaces, and core network elements, including circuit switched domain and packet switched (IP based) domain core network.

User Modeling in WCDMA is a major process in the dimensioning activities. With a given network setting (i.e., available spectrum, blocking probability, and BS characteristics) and a path loss model, the dimensioning activities determine the user distribution, which is essential for the accurate calculation of interference and mobility. User Modeling helps compute the traffic density in the cellular network, which can be used to optimize the placement of BSs and radio network controllers as well as to analyze the performance of resource management algorithms towards meeting the final goal: the calculation and maximization of network capacity.

3.2 Related Work

In the past decade, the problem of modeling user distribution and mobility has been an engaging research subject.

In [18], the authors propose a method for creating two layers of hierarchical cellular networks: Macrocell and Microcell to address high and low mobility of users. Microcells accommodate both new and handoff requests and can handle all types of high-rate connection requests, including voice, video, and data, while Macrocells, which have larger coverage, can be responsible for both new and handoff requests but have limited application capabilities, such as reduced quality video. This specific arrangement made the Macrocells encompass and lower the handoff rate for faster-moving users, while the Microcells can be deployed in hot-spot areas to provide high-rate services to stationary or slow-moving users.

In [22], the authors use dynamic pricing to regulate the demand on wireless services, as well as altering the mobility of users during peak time while also utilizing network resources during off-peak hours by lowering prices to the users.

In [44], the authors' model different aspects of user distribution and mobility by taking two new concepts into account: user classes and street types. With the ability to load real map data into numerical simulations, the software can calculate the network capacity and capture the movement of different user classes in the Helsinki area.

Recent research has looked at different aspects that contribute to user distribution and mobility, but most of it has focused on mobility and manually placing users in simulations. In [6], the authors show that user distribution does drastically affect the overall network capacity. This section will show that by using the 2D-Gaussian function at each BS, user distribution and interference can be easily modeled for many different scenarios, including users uniformly distributed, users densely clustered at the center of the cells, and users at the cells' boundaries.

3.3 User and Interference Model

This study assumes that each user is always communicating and is power controlled by the base station (BS) that has the highest received power at the user. Let $r_i(x, y)$ and $r_j(x, y)$

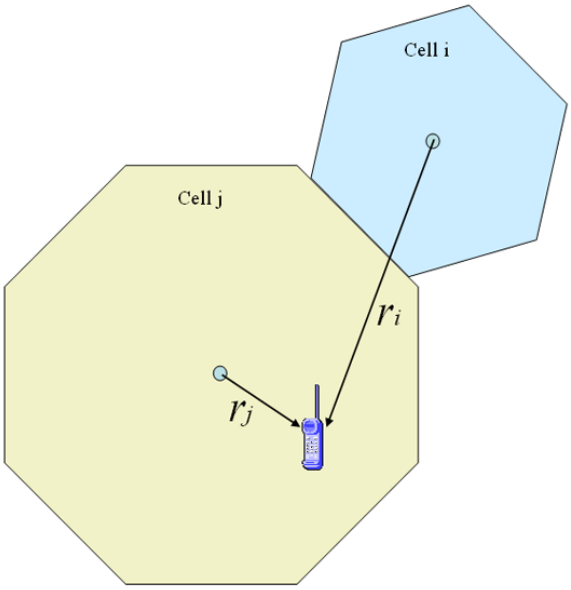

Figure 3.1: Inter-cell interference on cell i from users in cell j

be the distance from a user to BS i and BS j, respectively. This user is power controlled by BS j in the cell or region C_j with area A_j, which BS j services as showed in Fig. 3.1. This study assumes that both large scale path loss and shadow fading are compensated by the perfect power control mechanism. Let $I_{ji,g}$ be the average inter-cell interference that all users $n_{j,g}$ using services g with activity factor v_g and received signal S_g at BS j impose on BS i. Modifying the average inter-cell interference given by [5], the equation becomes [43]

$$I_{ji}^{(g)} = S_g v_g n_{j,g} \frac{e^{(\gamma\sigma_s)^2}}{A_j} \int\int_{C_j} \frac{r_j^m(x,y)}{r_i^m(x,y)} \, w(x,y) \, dA(x,y), \tag{3.1}$$

where $\gamma = \ln(10)/10$, σ_s is the standard deviation of the attenuation for the shadow fading, m is the path loss exponent, and $w(x,y)$ is the user distribution density at (x,y). Let $\kappa_{ji,g}$ be the per-user (with service g) relative inter-cell interference factor from cell j to BS i,

$$\kappa_{ji,g} = \frac{e^{(\gamma\sigma_s)^2}}{A_j} \int\int_{C_j} \frac{r_j^m(x,y)}{r_i^m(x,y)} \, w(x,y) \, dA(x,y). \tag{3.2}$$

The inter-cell interference density I_{ji}^{inter} from cell j to BS i from all services G becomes

$$I_{ji}^{inter} = \frac{1}{W} \sum_{g=1}^{G} I_{ji}^{(g)}, \tag{3.3}$$

where W is the bandwidth of the system. Eq. (3.3) can be rewritten as

$$I_{ji}^{inter} = \frac{1}{W} \sum_{g=1}^{G} S_g v_g \; n_{j,g} \; \kappa_{ji,g}. \tag{3.4}$$

Thus, the total inter-cell interference density I_i^{inter} from all other cells to BS i is

$$I_i^{inter} = \frac{1}{W} \sum_{j=1, j\neq i}^{M} \sum_{g=1}^{G} S_g v_g \; n_{j,g} \; \kappa_{ji,g}, \tag{3.5}$$

where M is the total number of cells in the network.

If the user distribution density can be approximated, then, $\kappa_{ji,g}$ needs to be calculated only once. The user distribution is modeled with a 2-dimensional Gaussian function as follows

$$w(x,y) = \frac{\eta}{2\pi\sigma_1\sigma_2} e^{-\frac{1}{2}(\frac{x-\mu_1}{\sigma_1})^2} e^{-\frac{1}{2}(\frac{y-\mu_2}{\sigma_2})^2}, \tag{3.6}$$

where η is a user density normalizing parameter.

By specifying the means μ_1 and μ_2 and the standard deviations σ_1 and σ_2 of the distribution for every cell, an approximation can be found for a wide range of user distributions ranging from uniform to hot-spot clusters. These results are compared with simulations to determine the value of η experimentally.

3.4 Numerical Results

The results shown are for a twenty-seven cell network topology used in [5, 6]. The COST-231 propagation model with a carrier frequency of 1800 MHz, average base station height of 30 meters and average mobile height of 1.5 meters, is used to determine the coverage region. The path loss coefficient m is 4. The shadow fading standard deviation σ_s is 6 dB. We assume only one service, i.e., $G = 1$. The processing gain $\frac{W}{R}$ is 21.1 dB. The activity factor, v, is 0.375.

The simulator used for comparison is an extension of the software tools CDMA Capacity Allocation and Planning (CCAP) [3]. CCAP, written in MATLAB, was developed at Washington University in St. Louis for numerical analysis of optimization techniques developed

in [5] to compute the capacity of CDMA networks. This study extends CCAP for WCDMA networks and uses the 2-dimensional Gaussian function for $w(x, y)$. The following models show that by using 2-D Gaussian distribution, many different scenarios can be modeled, including users uniformly distributed, users clustered at the center of the cells, and users at the cells' boundaries. The results are verified with [6], where actual distances were used to simulate real-time users entering the network for the calculation of interference.

3.4.1 Uniform Distribution of Users

The network with different values of σ_1 and σ_2 has been analyzed, while keeping μ_1 and μ_2 equal to zero in (3.6). Table 3.1 shows the maximum number of users in every cell for the 27 cell WCDMA network, as the values of σ_1 and σ_2 are increased from 5000 to 15000, while $\mu_1 = 0$ and $\mu_2 = 0$. These increments of σ_1, σ_2 result in users spread out, almost uniformly in the cells. Fig. 3.2 shows the 2-D Gaussian approximation of users uniformly distributed in the cells with $\sigma_1 = \sigma_2 = 12000$. The total number of users is 548. This compares well with simulation results presented in Fig. 3.3, which yields a total number of users equal to 554 when they are placed uniformly in the cells.

3.4.2 Users Densely Clustered at the Center of the Cells

Table 3.2 shows the maximum number of users in every cell for the 27-cell WCDMA network as the values of σ_1 and σ_2 are increased from 100 to 400 while $\mu_1 = 0$ and $\mu_2 = 0$. This results in users densely clustered around the BSs. Fig. 3.4 shows the 2-D Gaussian approximation with $\sigma_1 = \sigma_2 = 100$. The maximum number of users is 1026. This compares exactly with simulation results presented in Fig. 3.5, which also yields a total number of users equal to 1026. In this configuration, the users cause the least amount of interference to the network by reducing the power gain required to maintain a desired signal-to-noise ratio.

Table 3.1: The maximum number of users in every cell for the 27 cell WCDMA network (with σ_1 and σ_2 are increased from 5000 to 15000 while $\mu_1 = 0$ and $\mu_2 = 0$). This results in users distributed uniformly in all BSs.

$\sigma = \sigma_1, \sigma_2$	5000	7000	10000	12000	15000	Capacity from [5]
$Cell_1$	18	18	18	18	18	18
$Cell_2$	18	18	18	18	18	18
$Cell_3$	18	18	18	17	17	17
$Cell_4$	18	18	18	17	17	17
$Cell_5$	18	18	18	18	18	18
$Cell_6$	18	18	18	17	17	17
$Cell_7$	18	18	18	17	17	17
$Cell_8$	18	18	18	18	18	18
$Cell_9$	18	17	17	17	17	17
$Cell_{10}$	22	21	21	21	21	21
$Cell_{11}$	22	22	22	21	21	21
$Cell_{12}$	22	21	21	21	21	21
$Cell_{13}$	17	17	17	17	17	17
$Cell_{14}$	18	18	18	18	18	18
$Cell_{15}$	18	17	17	17	17	17
$Cell_{16}$	22	21	21	21	21	21
$Cell_{17}$	22	22	21	21	21	21
$Cell_{18}$	22	21	21	21	21	21
$Cell_{19}$	18	17	17	17	17	17
$Cell_{20}$	25	25	25	25	25	25
$Cell_{21}$	25	25	24	24	24	24
$Cell_{22}$	25	25	24	24	24	24
$Cell_{23}$	25	25	25	25	25	25
$Cell_{24}$	25	25	25	25	25	25
$Cell_{25}$	25	25	24	24	24	24
$Cell_{26}$	25	25	24	24	24	24
$Cell_{27}$	25	25	25	25	25	25
Total Users	565	558	553	548	548	548

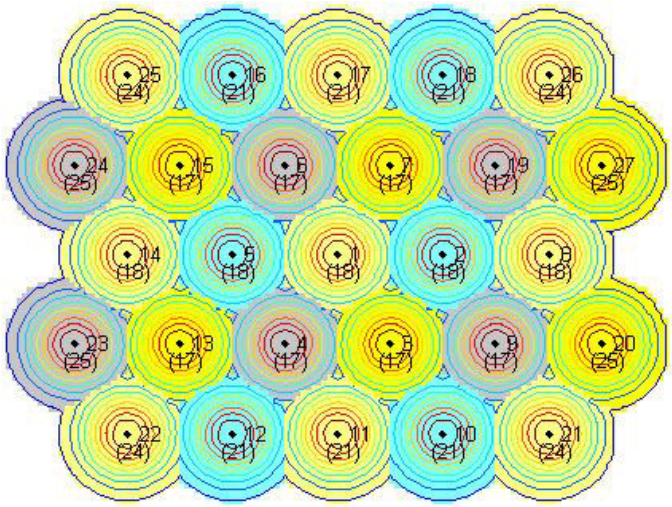

Figure 3.2: 2-D Gaussian approximation of users uniformly distributed in the cells. $\sigma_1 = \sigma_2 = 12000$, $\mu_1 = \mu_2 = 0$. The maximum number of users is 548.

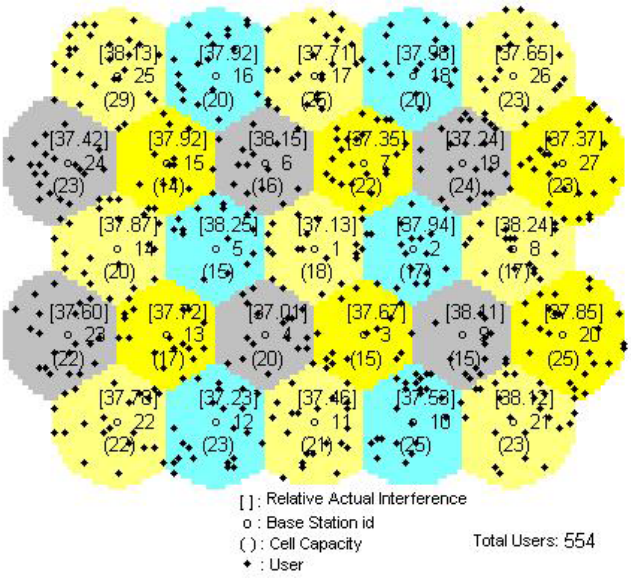

Figure 3.3: Simulated network capacity where users are uniformly distributed in the cells. The maximum number of users is 554.

Table 3.2: The maximum number of users in 27 cells of WCDMA network as the values of σ_1 and σ_2 are increased from 100 to 400 while $\mu_1 = 0$ and $\mu_2 = 0$. This results in users densely clustered around the BSs.

$\sigma = \sigma_1, \sigma_2$	$\sigma = 100$	$\sigma = 200$	$\sigma = 300$	$\sigma = 400$
$Cell_1$	38	38	37	34
$Cell_2$	38	38	37	34
$Cell_3$	38	38	37	35
$Cell_4$	38	38	37	35
$Cell_5$	38	38	37	34
$Cell_6$	38	38	37	35
$Cell_7$	38	38	37	35
$Cell_8$	38	38	37	35
$Cell_9$	38	38	37	35
$Cell_{10}$	38	38	37	36
$Cell_{11}$	38	38	37	36
$Cell_{12}$	38	38	37	36
$Cell_{13}$	38	38	37	35
$Cell_{14}$	38	38	37	35
$Cell_{15}$	38	38	37	35
$Cell_{16}$	38	38	37	35
$Cell_{17}$	38	38	37	35
$Cell_{18}$	38	38	37	35
$Cell_{19}$	38	38	37	35
$Cell_{20}$	38	38	37	36
$Cell_{21}$	38	38	38	36
$Cell_{22}$	38	38	38	37
$Cell_{23}$	38	38	38	36
$Cell_{24}$	38	38	38	36
$Cell_{25}$	38	38	37	36
$Cell_{26}$	38	38	37	36
$Cell_{27}$	38	38	37	36
Total Users	1026	1026	1003	954

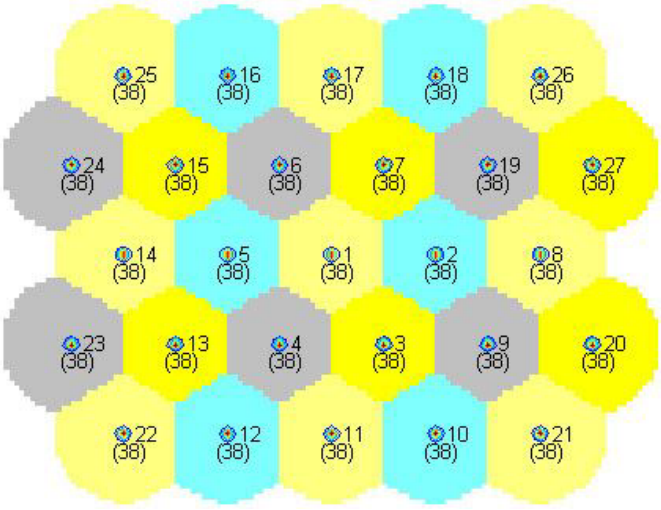

Figure 3.4: 2-D Gaussian approximation of users densely clustered around the BSs. $\sigma_1 = \sigma_2 = 100$, $\mu_1 = \mu_2 = 0$. The maximum number of users is 1026.

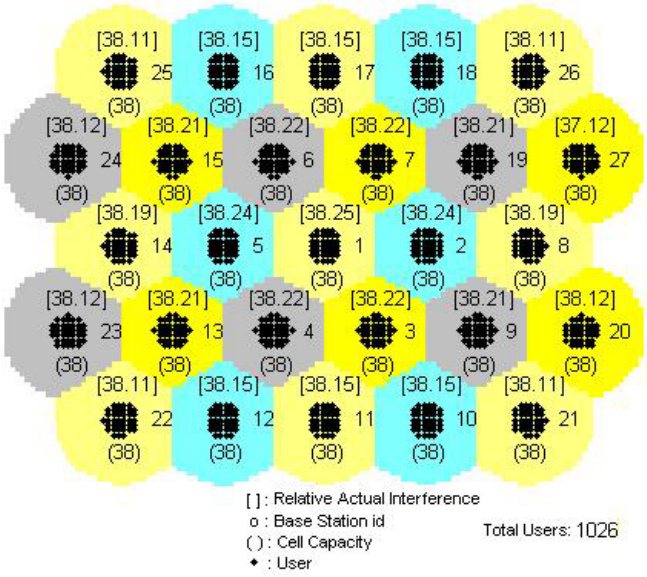

Figure 3.5: Simulated network capacity where users are densely clustered around the BSs causing the least amount of inter-cell interference. The maximum number of users is 1026 in the network.

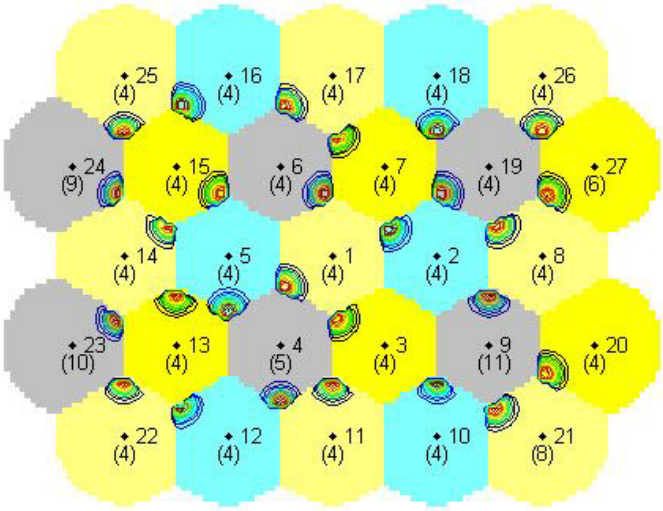

Figure 3.6: 2-D Gaussian approximation of users clustered at the boundaries of the cells. The values of σ_1, σ_2, μ_1, and μ_2 may be different in the different cells and are given in Table 3.3. The maximum number of users is 133.

3.4.3 Users Distributed at Cells' Boundaries

Fig. 3.6 shows the 2-D Gaussian approximation of users clustered at the boundaries of the cells. The values of σ_1, σ_2, μ_1, and μ_2 may be different in the different cells and are given in Table 3.3. The maximum number of users is 133. These results are close to what was attained through simulation. The maximum network capacity was purposely decreased by the simulator by placing the users so they caused the maximum interference to the network. The simulation yielded a total capacity of 108 users, with only 4 users in each cell. The pattern seen in Fig. 3.7 shows that the simulator placed the users at the extreme corners of their respective cells. The placement at extremities would require users to increase their power gain causing much more interference to other users.

Table 3.3: The values of σ_1, σ_2, μ_1, and μ_2 for the 2-D Gaussian approximation of users clustered at the boundaries of the cells as shown in Fig. 3.6. The maximum number of users is 133.

	μ_1	σ_1	μ_2	σ_2
$Cell_1$	-1400	300	-900	300
$Cell_2$	-1400	300	800	300
$Cell_3$	-1400	300	800	300
$Cell_4$	0	300	-1700	300
$Cell_5$	0	300	-1600	300
$Cell_6$	1300	300	-800	300
$Cell_7$	-1400	300	900	300
$Cell_8$	-1300	300	900	300
$Cell_9$	0	300	1500	300
$Cell_{10}$	0	300	1600	300
$Cell_{11}$	0	300	1550	300
$Cell_{12}$	-1400	300	900	300
$Cell_{13}$	0	300	1500	300
$Cell_{14}$	1300	300	900	300
$Cell_{15}$	1300	300	-800	300
$Cell_{16}$	-1350	300	-850	300
$Cell_{17}$	-1400	300	-900	300
$Cell_{18}$	0	300	-1600	300
$Cell_{19}$	-1400	300	-800	300
$Cell_{20}$	-1400	300	-800	300
$Cell_{21}$	-1350	300	800	300
$Cell_{22}$	0	300	1600	300
$Cell_{23}$	1350	300	800	300
$Cell_{24}$	1400	300	-800	300
$Cell_{25}$	0	300	-1700	300
$Cell_{26}$	0	300	-1600	300
$Cell_{27}$	-1350	300	-850	300

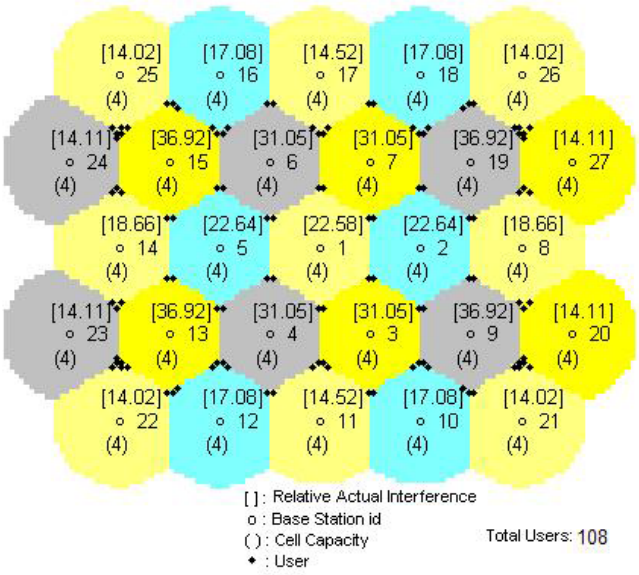

Figure 3.7: Simulated network capacity where users are clustered at the boundaries of the cells causing the most amount of inter-cell interference. The maximum number of users is only 108 in the network.

3.5 Conclusions

An analytical model has been presented for approximating the user distributions in multi-cell WCDMA networks using 2-dimensional Gaussian function by determining the means and the standard deviations of the distributions for every cell. This allowed for the calculation of the inter-cell interference and the reverse-link capacity of the network. The model compares well with simulation results and is fast and accurate enough to be used efficiently in the planning process of large WCDMA networks.

CHAPTER 4

WCDMA CAPACITY

4.1 Introduction

3G cellular systems are identified as International Mobile Telecommunications-2000 under International Telecommunication Union and as Universal Mobile Telecommunications Systems (UMTS) by European Telecommunications Standards Institute. Besides voice capability in 2G, the new 3G systems are required to have additional support on a variety of data-rate services using multiple access techniques. CDMA has been the fastest-growing digital wireless technology since its first commercialization in 1994. The major markets for CDMA are North America, Latin America, and Asia (particularly Japan and Korea). In total, CDMA has been adopted by more than 100 operators across 76 countries around the globe [16]. According to [25, 50], CDMA technology can offer about 7 to 10 times the capacity of analog technologies and up to 6 times the capacity of digital technologies such as TDMA. With its tremendous advantages such as voice quality, system reliability, and handset battery life compared to TDMA and FDMA technologies, WCDMA, the next generation of CDMA, is the best candidate for 3G cellular systems [29, 45].

4.2 Related Work

Since the first comparisons of multiple access schemes for UMTS [45], which found that WCDMA was well suited for supporting variable bit rate services, several study on WCDMA capacity has been considered.

In [79], the authors present a method to calculate the WCDMA reverse link Erlang capacity based on the Lost Call Held (LCH) model as described in [69]. This algorithm

calculates the occupancy distribution and capacity of UMTS/WCDMA systems based on a system outage condition. In this research, the authors derive a closed form expression of Erlang capacity for a single type of traffic loading and compare analytical results with simulations results.

The same LCH model was also used in [78] to calculate the forward link capacity of UMTS/WCDMA systems based on the system outage condition. In the forward link, because many users share the BS transmission power, the capacity is calculated at the BS. The transmission power from the BS is provided to each user based on each user's relative need. The access in the calculation of forward link capacity is one-to-many rather than many-to-one as in the reverse link. In this research, the authors provide capacity calculation results and performance evaluation through simulation.

An alternate approach, where MSs are synchronized on the uplink, i.e., signals transmitted from different MSs are time aligned at the BS, has been considered. Synchronous WCDMA looks at time synchronization for signal transmission between the BS and MS to improve network capacity. The performance of an uplink-synchronous WCDMA is analyzed in [14]. Scrambling codes are unique for each cell. MSs in the same cell share the same scrambling code, while different orthogonal channelization codes are derived from the set of Walsh codes. In [14], the potential capacity gain is about 35.8% in a multicell scenario with infinite number of channelization codes per cell and no soft handoff capability between MSs and BSs. However, the capacity gain in a more realistic scenario is reduced to 9.6% where soft handoff is enabled. The goal of this uplink-synchronous method in WCDMA is to reduce intra-cell interference. But the implementation is fairly complex while the potential capacity gain is not very high.

In this work, we will calculate the maximum reverse link capacity in UMTS/WCDMA systems for a set of quality of service requirements.

4.3 WCDMA Capacity with Perfect Power Control

In WCDMA, with perfect power control (PPC) between BSs and MSs, the energy per bit to total interference density at BS i for a service g is given by [43, 55]

$$\left(\frac{E_b}{I_0}\right)_{i,g} = \frac{\frac{S_g}{R_g}}{N_0 \ + \ I_i^{inter} \ + \ I_i^{own} \ - \ S_g v_g}, \tag{4.1}$$

where N_0 is the thermal noise density, and R_g is the bit rate for service g. I_i^{inter} was calculated in section 3.3. I_i^{own} is the total intra-cell interference density caused by all users in cell i. Thus I_i^{own} is given by

$$I_i^{own} = \frac{1}{W} \sum_{g=1}^{G} \ S_g v_g n_{i,g}. \tag{4.2}$$

Let τ_g be the minimum signal-to-noise ratio, which must received at a BS to decode the signal of a user with service g, and S_g^* be the maximum signal power, which the user can transmit. Substituting (3.5) and (4.2) into (4.1), we have for every cell i in the WCDMA network, the number of users $n_{i,g}$ in BS i for a given service g needs to meet the following inequality constraint

$$\tau_g \leq \frac{\frac{S_g^*}{R_g}}{N_0 + \frac{S_g^*}{W}\left[\sum\limits_{g=1}^{G} \ n_{i,g} v_g + \sum\limits_{j=1, j\neq i}^{M} \sum\limits_{g=1}^{G} n_{j,g} v_g \kappa_{ji,g} - v_g\right]}, \text{ for } i\text{=1, ...,}M. \tag{4.3}$$

After rearranging terms, (4.3) can be rewritten as

$$\sum_{g=1}^{G} \ n_{i,g} v_g + \sum_{j=1, j\neq i}^{M} \sum_{g=1}^{G} n_{j,g} v_g \kappa_{ji,g} - v_g \leq c_{eff}^{(g)}, \text{ for } i\text{=1, ...,}M, \tag{4.4}$$

where

$$c_{eff}^{(g)} = \frac{W}{R_g}\left[\frac{1}{\tau_g} - \frac{R_g}{S_g^*/N_0}\right]. \tag{4.5}$$

The capacity in a WCDMA network is defined as the maximum number of simultaneous users $(n_{1,g}, n_{2,g}, ..., n_{M,g})$ for all services $g = 1, ..., G$ that satisfy (4.4).

4.4 WCDMA Capacity with Imperfect Power Control

The calculation of WCDMA network capacity, which was formulated in section 4.3, assumes perfect power control between the BSs and MSs. However, transmitted signals between BSs and MSs are subject to multipath propagation conditions, which make the received $\left(\frac{E_b}{I_o}\right)_{i,g}$ signals vary according to a log-normal distribution with a standard deviation on the order of 1.5 to 2.5 dB [69]. Thus, in the imperfect power control (IPC) case, the constant value of $(E_b)_{i,g}$ in each cell i for every user with service g needs to be replaced by the variable $(E_b)_{i,g} \triangleq \epsilon_{i,g}(E_b)_{o,g}$, which is log-normally distributed. We define

$$x_{i,g} = 10\log_{10}\left(\frac{\epsilon_{i,g}(E_b)_{o,g}}{I_0}\right), \tag{4.6}$$

to be a normally distributed random variable with mean m_c and standard deviation σ_c. Hence, inverting (4.6), we have

$$\frac{(E_b)_{o,g}}{I_0}\epsilon_{i,g} = 10^{x_{i,g}/10} = e^{\beta x_{i,g}}, \tag{4.7}$$

where $\beta = \ln(10)/10$.

According to [69], by evaluating the nth moment of $\epsilon_{i,g}$ using the fact that $x_{i,g}$ is Gaussian with mean m_c and standard deviation σ_c, then taking the average value (the expected value), we have

$$E\left[10^{(x_{i,g}/10)}\right] = E\left[\frac{(E_b)_{o,g}}{I_0}\epsilon_{i,g}\right] = \frac{(E_b)_{o,g}}{I_0}\ E[\epsilon_{i,g}] = e^{\beta m_c}\ e^{\frac{(\beta\sigma_c)^2}{2}}. \tag{4.8}$$

We can choose $\frac{(E_b)_{o,g}}{I_0}$ such that

$$\frac{(E_b)_{o,g}}{I_0} = e^{\beta m_c} = 10^{m_c/10}, \tag{4.9}$$

which makes

$$\frac{(E_b)_{o,g}}{I_0} = \text{median}\left[\left(\frac{E_b}{I_0}\right)_{i,g}\right], \tag{4.10}$$

for every user with service g in cell i.

Thus, the expected value becomes

$$E\left[\frac{(E_b)_{o,g}}{I_0}\epsilon_{i,g}\right] = \frac{(E_b)_{i,g}}{I_0}\ e^{\frac{(\beta\sigma_c)^2}{2}}. \tag{4.11}$$

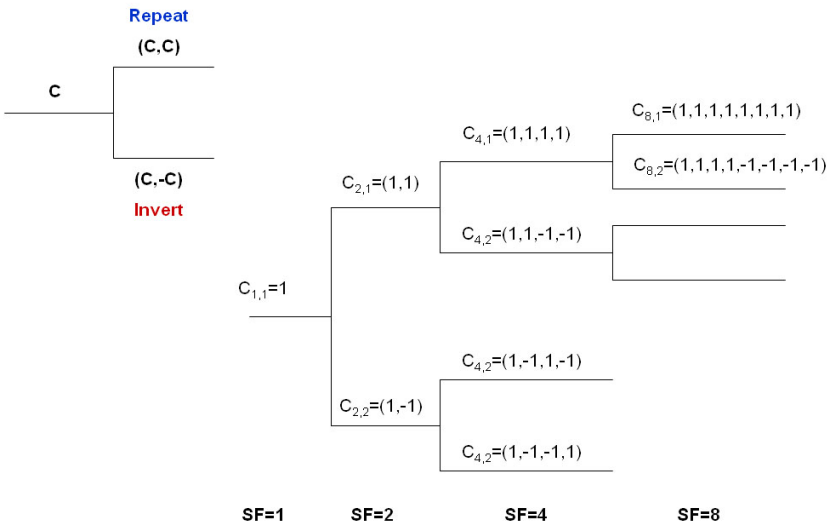

Figure 4.1: Generation of OVSF codes for different Spreading Factors.

As a result of (4.11), $c^{(g)}_{eff\_IPC}$ becomes $c^{(g)}_{eff}$ / $e^{\frac{(\beta\sigma_C)^2}{2}}$.

4.5 Spreading and Scrambling

Communication from a single source is separated by channelization codes, i.e., the dedicated physical channel in the uplink and the downlink connections within one sector from one MS. The Orthogonal Variable Spreading Factor (OVSF) codes, which were originally introduced in [21], were used to be channelization codes for UMTS.

The use of OVSF codes allows the orthogonality and spreading factor (SF) to be changed between different spreading codes of different lengths. Fig. 4.1 depicts the generation of different OVSF codes for different SF values.

The data signal after spreading is then scrambled with a scrambling codes to separate MSs and BSs from each other. Scrambling is used on top of spreading, thus it only makes the signals from different sources distinguishable from each other. Fig. 4.2 depicts the relationship between the spreading and scrambling process. Table 4.1 describes the different functionality of the channelization and the scrambling codes.

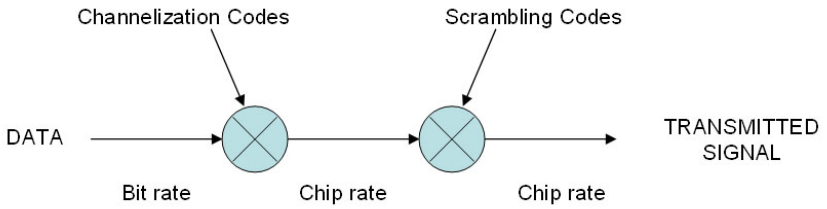

Figure 4.2: Relationship between spreading and scrambling.

Table 4.1: Functionality of the channelization and scrambling codes.

	Channelization code	Scrambling code
Usage	Uplink: Separation of physical data (DPDCH) and control channels (DPCCH) from same MS Downlink: Separation of downlink connections to different MSs within one cell.	Uplink: Separation of MSs Downlink: Separation of sectors (cells)
Length	Uplink: 4-256 chips same as SF Downlink 4-512 chips same as SF	Uplink: 10 ms = 38400 chips Downlink: 10 ms = 38400 chips
Number of codes	Number of codes under one scrambling code = spreading factor	Uplink: Several millions Downlink: 512
Code family	Orthogonal Variable Spreading Factor	Long 10 ms code: Gold Code Short code: Extended S(2) code family
Spreading	Yes, increases transmission bandwidth	No, does not affect transmission bandwidth

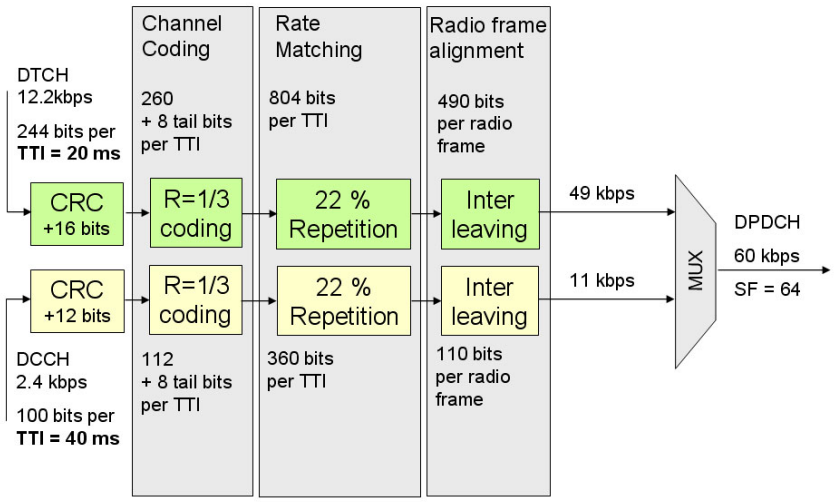

Figure 4.3: 12.2 Kbps Uplink Reference channel.

The typical required data rate or Dedicated Traffic Channel (DTCH) for a voice user is 12.2 Kbps. However, the Dedicated Physical Data Channel (DPDCH), which is the actual transmitted data rate, is dramatically increased due to the incorporated Dedicated Control Channel (DCCH) information, and the processes of Channel Coding, Rate Matching, and Radio Frame Alignment. Fig. 4.3 depicts the process of creating the actual transmitted signal for a voice user. Fig. 4.4 shows the DPDCH data rate requirement for 64 Kbps data user. Table 4.2 shows the approximation of the maximum user data rate with $\frac{1}{2}$ rate coding for different values of DPDCH.

4.6 Numerical Results

The results shown are for a twenty-seven cell network topology used in [2, 5, 6, 43]. The COST-231 propagation model with a carrier frequency of 1800 MHz, average base station height of 30 meters and average mobile height of 1.5 meters, is used to determine the coverage region. The path loss coefficient m is 4. The shadow fading standard deviation σ_s is 6 dB. The processing gain $\frac{W}{R_g}$ is 6.02 dB, 12.04 dB, 18.06 dB, and 24.08 dB for Spreading Factor

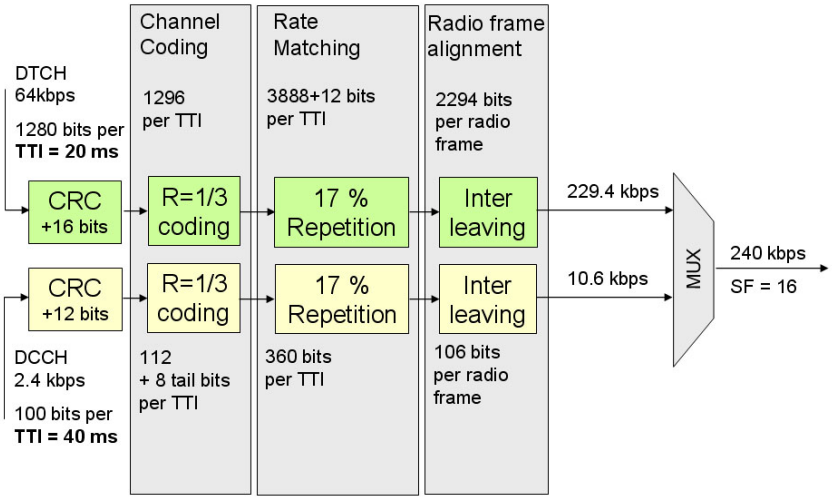

Figure 4.4: 64 Kbps Uplink Reference channel.

Table 4.2: Uplink DPDCH data rates.

DPDCH Spreading Factor	DPDCH channel bit rate (Kbps)	Maximum user data rate with $\frac{1}{2}$ rate coding (approx.)
256	15	7.5 Kbps
128	30	15 Kbps
64	60	30 Kbps
32	120	60 Kbps
16	240	120 Kbps
8	480	240 Kbps
4	960	480 Kbps
4, with 6 parallel codes	5740	2.8 Mbps

equal to 4, 16, 64, and 256, respectively. The activity factor, v, is 0.375.

This study extends the software tools (CCAP) [3] to analyze different SF in WCDMA networks. CCAP, written in MATLAB, was developed at Washington University in St. Louis for numerical analysis of optimization techniques developed in [5] to compute the capacity of CDMA networks.

The WCDMA network with 27 omni-directional antenna cells (1 sector per cell) was analyzed for evaluation of capacity using user modeling with the 2-D Gaussian function, whose parameters were determined in Chap. 3, and traditional methods of modeling uniform user distribution. The network with different values for $\frac{E_b}{I_0}$ was analyzed for different SF values of 4, 16, 64, and 256.

4.6.1 WCDMA Capacity Optimization with SF of 256

First, we set SF to 256, which is used to carry data for the control channel. Table 4.3 shows the number of slots per cell with omni-directional antenna for the scenario with $\frac{E_b}{I_0} = 7.5$ dB while the standard deviation of the imperfect power control is increased from 0 to 2.5 dB. Fig. 4.5 shows the optimized average number of slots per sector for the 27 cells WCDMA network as the $\frac{E_b}{I_0}$ is increased from 5 dB to 10 dB and the standard deviation of imperfect power control is increased from 0 to 2.5 dB. Because of IPC, to get the same average number of slots per sector as PPC, we have to decrease the SIR threshold by 0.5 dB to 1.5 dB. Fig. 4.5 also shows that the traditional uniform user distribution modeling matches well with the 2-D Gaussian model.

4.6.2 WCDMA Capacity Optimization with SF of 64

Next, we set SF to 64, which is used for voice communication as shown in Fig. 4.3. As a result of lowering the SF to 64, the number of slots per sector decreases by almost a factor of 4 compared to SF equal 256 (from 60.58 to 15.56 slots when $\frac{E_b}{I_o} = 7.5$ dB in PPC). Table

Table 4.3: Capacity calculation for uniform user distribution with SF = 256 and $\frac{E_b}{I_o}$ = 7.5 dB.

User Modeling with	2-D Gaussian function			Uniform User Distribution		
Imperfect Power Control. σ:	0.0	1.5	2.5	0.0	1.5	2.5
c_{eff}	110.20	97.92	79.40	110.20	97.92	79.40
$Cell_1$	52.86	46.97	38.09	52.67	46.80	37.95
$Cell_2$	53.95	47.94	38.87	53.79	47.80	38.75
$Cell_3$	51.84	46.07	37.35	51.64	45.88	37.20
$Cell_4$	51.84	46.07	37.35	51.64	45.88	37.20
$Cell_5$	53.95	47.94	38.87	53.79	47.80	38.75
$Cell_6$	51.85	46.07	37.36	51.64	45.88	37.20
$Cell_7$	51.84	46.07	37.35	51.64	45.88	37.20
$Cell_8$	53.00	47.10	38.19	52.74	46.86	38.00
$Cell_9$	50.73	45.08	36.55	50.49	44.87	36.38
$Cell_{10}$	62.74	55.75	45.20	62.51	55.54	45.04
$Cell_{11}$	63.29	56.24	45.60	63.08	56.05	45.45
$Cell_{12}$	62.73	55.74	45.20	62.51	55.54	45.04
$Cell_{13}$	50.73	45.08	36.55	50.49	44.87	36.38
$Cell_{14}$	53.01	47.10	38.19	52.74	46.86	38.00
$Cell_{15}$	50.73	45.08	36.55	50.49	44.87	36.38
$Cell_{16}$	62.71	55.72	45.18	62.51	55.54	45.04
$Cell_{17}$	63.27	56.22	45.59	63.08	56.05	45.45
$Cell_{18}$	62.71	55.73	45.19	62.51	55.54	45.04
$Cell_{19}$	50.74	45.08	36.56	50.49	44.87	36.38
$Cell_{20}$	73.40	65.22	52.88	73.26	65.10	52.78
$Cell_{21}$	71.84	63.84	51.76	71.65	63.66	51.62
$Cell_{22}$	71.86	63.85	51.77	71.65	63.66	51.62
$Cell_{23}$	73.43	65.24	52.90	73.26	65.10	52.78
$Cell_{24}$	73.43	65.25	52.91	73.26	65.10	52.78
$Cell_{25}$	71.83	63.83	51.75	71.65	63.66	51.62
$Cell_{26}$	71.82	63.81	51.74	71.65	63.66	51.62
$Cell_{27}$	73.40	65.22	52.89	73.26	65.10	52.78
Network Capacity	1635.54	1453.29	1178.41	1630.06	1448.42	1174.46
Average Capacity per Sector	60.58	54.09	43.64	60.37	53.65	43.50

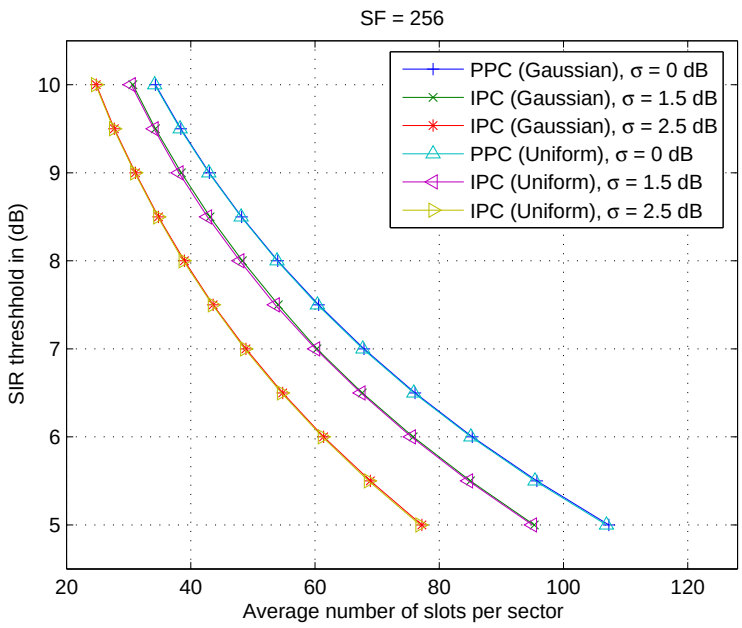

Figure 4.5: Average number of slot per sector for perfect and imperfect power control analysis with a Spreading Factor of 256.

4.4 shows the number of slots per cell for the scenario with $\frac{E_b}{I_0} = 7.5$ dB while the standard deviation of the imperfect power control is increased from 0 to 2.5 dB. Fig. 4.6 shows the optimized average number of slots per sector for the 27 cells WCDMA network as the $\frac{E_b}{I_0}$ is increased from 5 dB to 10 dB and the standard deviation of imperfect power control is increased from 0 to 2.5 dB. Because of IPC, to get the same amount of the average number of slots per sector as PPC, the SIR threshold has to be decreased by 0.5 dB to 1.5 dB. Fig. 4.6 also shows that the traditional uniform user distribution modeling matches well with the 2-D Gaussian model.

4.6.3 WCDMA Capacity Optimization with SF of 16

Next, we set SF to 16, which is used for 64 Kbps data communication as shown in Fig. 4.4. As a result of lowering the SF to 16, the number of slots per sector decreases by almost a factor of 4 compared to SF equal 64 (from 15.56 to 4.30 slots when $\frac{E_b}{I_o} = 7.5$ dB in PPC).

Table 4.4: Capacity calculation for uniform user distribution with SF = 64 and $\frac{E_b}{I_o}$ = 7.5 dB.

User Modeling with	2-D Gaussian function			Uniform User Distribution		
Imperfect Power Control. σ:	0.0	1.5	2.5	0.0	1.5	2.5
c_{eff}	28.30	25.23	20.60	28.30	25.23	20.60
$Cell_1$	13.58	12.10	9.88	13.53	12.06	9.85
$Cell_2$	13.86	12.35	10.09	13.82	12.32	10.06
$Cell_3$	13.32	11.87	9.69	13.26	11.82	9.65
$Cell_4$	13.32	11.87	9.69	13.26	11.82	9.65
$Cell_5$	13.86	12.35	10.09	13.82	12.32	10.06
$Cell_6$	13.32	11.87	9.69	13.26	11.82	9.65
$Cell_7$	13.32	11.87	9.69	13.26	11.82	9.65
$Cell_8$	13.61	12.14	9.91	13.54	12.08	9.86
$Cell_9$	13.03	11.62	9.48	12.97	11.56	9.44
$Cell_{10}$	16.11	14.37	11.73	16.06	14.31	11.69
$Cell_{11}$	16.26	14.49	11.83	16.20	14.44	11.79
$Cell_{12}$	16.11	14.36	11.73	16.06	14.31	11.69
$Cell_{13}$	13.03	11.62	9.48	12.97	11.56	9.44
$Cell_{14}$	13.62	12.14	9.91	13.54	12.08	9.86
$Cell_{15}$	13.03	11.62	9.48	12.97	11.56	9.44
$Cell_{16}$	16.11	14.36	11.72	16.06	14.31	11.69
$Cell_{17}$	16.25	14.49	11.83	16.20	14.44	11.79
$Cell_{18}$	16.11	14.36	11.72	16.06	14.31	11.69
$Cell_{19}$	13.03	11.62	9.49	12.97	11.56	9.44
$Cell_{20}$	18.85	16.81	13.72	18.82	16.78	13.70
$Cell_{21}$	18.45	16.45	13.43	18.40	16.41	13.39
$Cell_{22}$	18.46	16.45	13.43	18.40	16.41	13.39
$Cell_{23}$	18.86	16.81	13.73	18.82	16.78	13.70
$Cell_{24}$	18.86	16.81	13.73	18.82	16.78	13.70
$Cell_{25}$	18.45	16.45	13.43	18.40	16.41	13.39
$Cell_{26}$	18.45	16.44	13.43	18.40	16.41	13.39
$Cell_{27}$	18.85	16.81	13.72	18.82	16.78	13.70
Network Capacity	420.07	374.50	305.77	418.67	373.25	304.75
Average Capacity per Sector	15.56	13.87	11.32	15.51	13.82	11.29

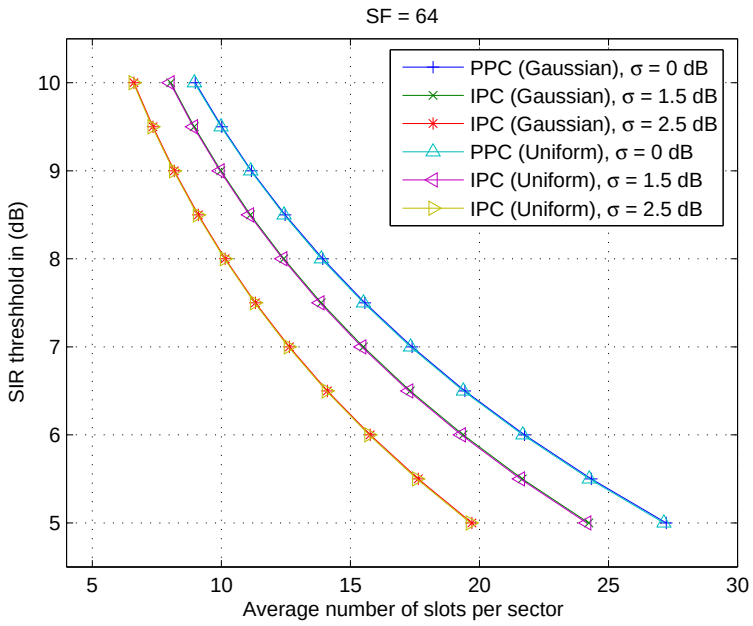

Figure 4.6: Average number of slot per sector for perfect and imperfect power control analysis with a Spreading Factor of 64.

Table 4.5 shows the number of slots per cell for the scenario with $\frac{E_b}{I_0} = 7.5$ dB while the standard deviation of the imperfect power control is increased from 0 to 2.5 dB. Fig. 4.7 shows the optimized average number of slots per sector for the 27 cells WCDMA network as the $\frac{E_b}{I_0}$ is increased from 5 dB to 10 dB and the standard deviation of imperfect power control is increased from 0 to 2.5 dB. Because of IPC, to get the same average number of slots per sector as PPC, we have to increase the SIR threshold by 0.5 dB to 1.5 dB. Fig. 4.7 also shows that the traditional uniform user distribution modeling matches well with the 2-D Gaussian model.

4.6.4 WCDMA Capacity Optimization with SF of 4

Next, we set SF to 4, which is used for 256 Kbps data communication between BSs and MSs. As a result of lowering the SF to 4, the number of slots per sector decreases significantly to 1.49 while keeping $\frac{E_b}{I_o} = 7.5$ dB in PPC. Table 4.6 shows the number of slots per cell for the

Table 4.5: Capacity calculation for uniform user distribution with SF = 16 and $\frac{E_b}{I_o}$ = 7.5 dB.

User Modeling with	2-D Gaussian function			Uniform User Distribution		
Imperfect Power Control. σ:	0.0	1.5	2.5	0.0	1.5	2.5
c_{eff}	7.83	7.06	5.90	7.83	7.06	5.90
$Cell_1$	3.75	3.39	2.83	3.74	3.37	2.82
$Cell_2$	3.83	3.46	2.89	3.82	3.45	2.88
$Cell_3$	3.68	3.32	2.78	3.67	3.31	2.77
$Cell_4$	3.68	3.32	2.78	3.67	3.31	2.77
$Cell_5$	3.83	3.46	2.89	3.82	3.45	2.88
$Cell_6$	3.68	3.32	2.78	3.67	3.31	2.77
$Cell_7$	3.68	3.32	2.78	3.67	3.31	2.77
$Cell_8$	3.76	3.40	2.84	3.75	3.38	2.82
$Cell_9$	3.60	3.25	2.72	3.59	3.23	2.70
$Cell_{10}$	4.46	4.02	3.36	4.44	4.00	3.35
$Cell_{11}$	4.50	4.05	3.39	4.48	4.04	3.38
$Cell_{12}$	4.46	4.02	3.36	4.44	4.00	3.35
$Cell_{13}$	3.60	3.25	2.72	3.59	3.23	2.70
$Cell_{14}$	3.77	3.40	2.84	3.75	3.38	2.82
$Cell_{15}$	3.60	3.25	2.72	3.59	3.23	2.70
$Cell_{16}$	4.45	4.02	3.36	4.44	4.00	3.35
$Cell_{17}$	4.49	4.05	3.39	4.48	4.04	3.38
$Cell_{18}$	4.45	4.02	3.36	4.44	4.00	3.35
$Cell_{19}$	3.60	3.25	2.72	3.59	3.23	2.70
$Cell_{20}$	5.21	4.70	3.93	5.20	4.69	3.92
$Cell_{21}$	5.10	4.60	3.85	5.09	4.59	3.84
$Cell_{22}$	5.10	4.60	3.85	5.09	4.59	3.84
$Cell_{23}$	5.22	4.70	3.93	5.20	4.69	3.92
$Cell_{24}$	5.22	4.70	3.93	5.20	4.69	3.92
$Cell_{25}$	5.10	4.60	3.85	5.09	4.59	3.84
$Cell_{26}$	5.10	4.60	3.85	5.09	4.59	3.84
$Cell_{27}$	5.21	4.70	3.93	5.20	4.69	3.92
Network Capacity	116.16	104.77	87.59	115.77	104.42	87.29
Average Capacity per Sector	4.30	3.88	3.24	4.29	3.87	3.23

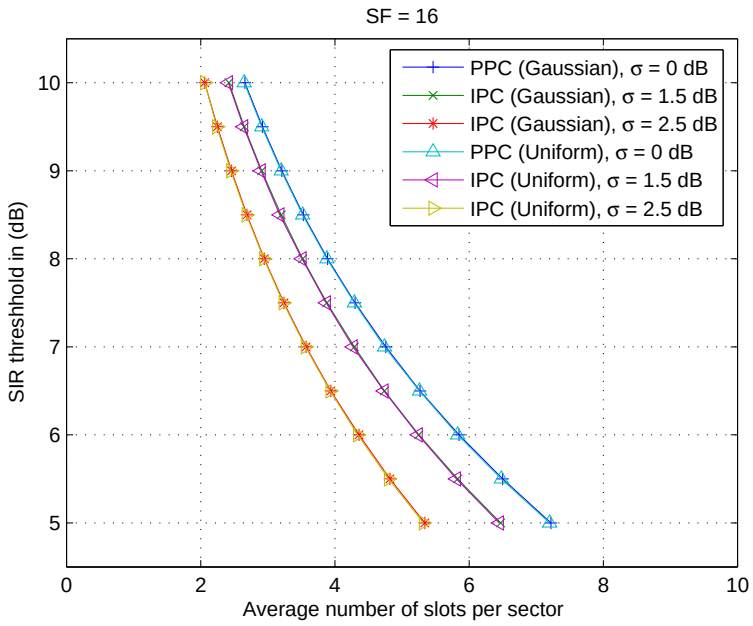

Figure 4.7: Average number of slot per sector for perfect and imperfect power control analysis with a Spreading Factor of 16.

scenario with $\frac{E_b}{I_0} = 7.5$ dB while the standard deviation of the imperfect power control is increased from 0 to 2.5 dB. Fig. 4.8 shows the optimized average number of slots per sector for the 27 cells WCDMA network as the $\frac{E_b}{I_0}$ is increased from 5 dB to 10 dB and the standard deviation of imperfect power control is increased from 0 to 2.5 dB. The results matches the previous trends for higher spreading factors.

4.7 Conclusions

An analytical model has been presented for optimizing capacity in multi-cell WCDMA networks. Numerical results show that the SIR threshold for the received signals is decreased by 0.5 to 1.5 dB due to the imperfect power control. As expected, we can have many low rate voice users or fewer data users as the data rate increases. The results also show that the determined parameters of the 2-dimensional Gaussian model matches well with traditional

Table 4.6: Capacity calculation for uniform user distribution with SF = 4 and $\frac{E_b}{I_o}$ = 7.5 dB.

User Modeling with	2-D Gaussian function			Uniform User Distribution		
Imperfect Power Control. σ:	0.0	1.5	2.5	0.0	1.5	2.5
c_{eff}	2.71	2.52	2.23	2.71	2.52	2.23
$Cell_1$	1.30	1.21	1.07	1.29	1.20	1.06
$Cell_2$	1.33	1.23	1.09	1.32	1.23	1.09
$Cell_3$	1.27	1.18	1.05	1.27	1.18	1.04
$Cell_4$	1.27	1.18	1.05	1.27	1.18	1.04
$Cell_5$	1.33	1.23	1.09	1.32	1.23	1.09
$Cell_6$	1.27	1.18	1.05	1.27	1.18	1.04
$Cell_7$	1.27	1.18	1.05	1.27	1.18	1.04
$Cell_8$	1.30	1.21	1.07	1.30	1.20	1.07
$Cell_9$	1.25	1.16	1.02	1.24	1.15	1.02
$Cell_{10}$	1.54	1.43	1.27	1.54	1.43	1.26
$Cell_{11}$	1.55	1.44	1.28	1.55	1.44	1.27
$Cell_{12}$	1.54	1.43	1.27	1.54	1.43	1.26
$Cell_{13}$	1.25	1.16	1.02	1.24	1.15	1.02
$Cell_{14}$	1.30	1.21	1.07	1.30	1.20	1.07
$Cell_{15}$	1.25	1.16	1.02	1.24	1.15	1.02
$Cell_{16}$	1.54	1.43	1.27	1.54	1.43	1.26
$Cell_{17}$	1.55	1.44	1.28	1.55	1.44	1.27
$Cell_{18}$	1.54	1.43	1.27	1.54	1.43	1.26
$Cell_{19}$	1.25	1.16	1.02	1.24	1.15	1.02
$Cell_{20}$	1.80	1.68	1.48	1.80	1.67	1.48
$Cell_{21}$	1.76	1.64	1.45	1.76	1.64	1.45
$Cell_{22}$	1.77	1.64	1.45	1.76	1.64	1.45
$Cell_{23}$	1.80	1.68	1.48	1.80	1.67	1.48
$Cell_{24}$	1.80	1.68	1.48	1.80	1.67	1.48
$Cell_{25}$	1.76	1.64	1.45	1.76	1.64	1.45
$Cell_{26}$	1.76	1.64	1.45	1.76	1.64	1.45
$Cell_{27}$	1.80	1.68	1.48	1.80	1.67	1.48
Network Capacity	40.18	37.33	33.03	40.04	37.20	32.92
Average Capacity per Sector	1.49	1.38	1.22	1.48	1.38	1.22

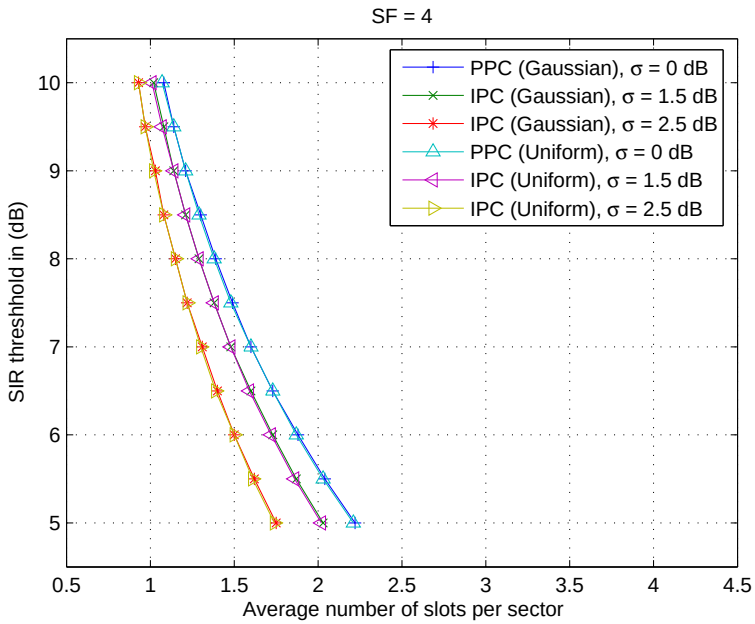

Figure 4.8: Average number of slot per sector for perfect and imperfect power control analysis with a Spreading Factor of 4.

methods for modeling uniform user distribution. Our method of optimizing capacity is fast, accurate, and can be implemented for large multi-cell WCDMA networks.

CHAPTER 5

WCDMA CALL ADMISSION CONTROL AND THROUGHPUT

5.1 Introduction

Call admission control (CAC) algorithms, in general, decide whether a new connection could be admitted without impacting the quality of service (QoS) of current connections in a network. In addition, CAC algorithms must be designed to fulfill a grade of service (GoS), i.e., call blocking rate. The existence of CAC algorithms in mobile phone systems protects the cellular network and users while achieving network performance objectives.

A CAC algorithm is considered global if the decision to admit a call is based on the current total number of calls in the entire network, and local if the algorithm considers only a single cell for making that decision. A global CAC is most often a centralized scheme while a local CAC is distributed in nature. Each approach has advantages and disadvantages. In this chapter, we design a CAC algorithm for multi-cell WCDMA networks and analyze its complexity, implementation, and performance.

5.2 Feasible States

Recall from section 4.3 that the number of calls in every cell must satisfy

$$\sum_{g=1}^{G} n_{i,g} v_g + \sum_{j=1, j\neq i}^{M} \sum_{g=1}^{G} n_{j,g} v_g \kappa_{ji,g} - v_g \leq c_{eff}^{(g)} \quad \text{for } i{=}1..M, \tag{5.1}$$

where

$$c_{eff}^{(g)} = \frac{W}{R_g}\left[\frac{1}{\tau_g} - \frac{R_g}{S_g^*/N_0}\right]. \tag{5.2}$$

A set of calls $\mathbf{n} = \begin{bmatrix} n_{1,1} & \dots & n_{1,G} \\ \dots & \dots & \dots \\ n_{M,1} & \dots & n_{M,G} \end{bmatrix}$ satisfying the above equations is said to be in feasible call configuration or a feasible state, which meet the $\frac{E_b}{I_0}$ constraint.

Denote by Ω the set of feasible states. Define the set of blocking states for service g in cell i as

$$\mathcal{B}_{i,g} = \left\{ \mathbf{n} \in \Omega : \begin{bmatrix} n_{1,1} & \dots & n_{1,g} & \dots & n_{1,G} \\ \dots & \dots & \dots & \dots & \dots \\ n_{i,1} & \dots & n_{i,g} & \dots & n_{i,G} \\ \dots & \dots & \dots & \dots & \dots \\ n_{M,1} & \dots & n_{M,g} & \dots & n_{M,G} \end{bmatrix} \notin \Omega \right\}. \tag{5.3}$$

If a new connection or a handoff connection with the service g arrives to cell i, it is blocked when the current state of the network, $\mathbf{n}$, is in $\mathcal{B}_{i,g}$.

5.3 Mobility Model

The call arrival process with service g to cell i is assumed to be a Poisson process with rate $\lambda_{i,g}$ independent of other call arrival processes. The call dwell time is a random variable with exponential distribution having mean $1/\mu$, and it is independent of earlier arrival times, call durations and elapsed times of other users. At the end of a dwell time a call may stay in the same cell, attempt a handoff to an adjacent cell, or leave the network. Define $q_{ii,g}$ as the probability that a call with service g in progress in cell i remains in cell i after completing its dwell time. In this case, a new dwell time that is independent of the previous dwell time begins immediately. Let $q_{ij,g}$ be the probability that a call with service g in progress in cell i after completing its dwell time goes to cell j. If cells i and j are not adjacent, then $q_{ij,g} = 0$ ($\forall\ g\ \in\ G$). We denote by $q_{i,g}$ the probability that a call with service g in progress in cell i departs from the network.

This mobility model is attractive because we can easily define different mobility scenarios by varying the values of these probability parameters [65]. For example, if $q_{i,g}$ is constant for all i and g, then the average dwell time of a call of the same service in the network will be constant regardless of where the call originates and what the values of $q_{ii,g}$ and $q_{ij,g}$ are. Thus, by varying $q_{ii,g}$'s and $q_{ij,g}$'s for a service g, we can obtain low and high mobility scenarios and compare the effect of mobility on network attributes (e.g., throughput).

We assume that the occupancy of the cells evolves according to a birth-death process, where the total arrival rate or offered traffic for service g to cell i is $\rho_{i,g}$, and the departure rate from cell i when the network is in state $\mathbf{n}$ is $n_{i,g}\mu_{i,g} = n_{i,g}\mu(1 - q_{ii,g})$. Let ρ be the matrix of offered traffic of service g to the cells, μ the matrix of departure rates, and let $p(\rho, \mu, \mathbf{n})$ be the stationary probability that the network is in state $\mathbf{n}$. The distribution p is obtained as follows

$$p(\rho,\mu,\mathbf{n}) = \begin{cases} P_0 \prod_{k=1}^{M}\prod_{g=1}^{G} \frac{(\rho_{k,g}/\mu_{k,g})^{n_{k,g}}}{n_{k,g}!} & \sum_{g=1}^{G} n_{i,g}v_g + \sum_{j=1,j\neq i}^{M}\sum_{g=1}^{G} n_{j,g}v_g\kappa_{ji,g} - v_g \leq c_{eff}^{(g)}, \\ & \text{for} \quad i = 1, ..., M, \\ 0 & \text{otherwise}, \end{cases} \tag{5.4}$$

where P_0 is a normalizing constant such that $\sum_{\mathbf{n}\in\Omega} p(\rho, \mu, \mathbf{n}) = 1$. The new call blocking probability for service g in cell i, $B_{i,g}$, is given by

$$B_{i,g} = \sum_{\mathbf{n}\in\mathcal{B}_{i,g}} p(\rho, \mu, \mathbf{n}). \tag{5.5}$$

This is also the blocking probability of handoff calls due to the fact that handoff calls and new calls are treated in the same way by the network.

Let $\mathcal{A}_i$ be the set of cells adjacent to cell i. Let $\nu_{ji,g}$ be the handoff rate out of cell j offered to cell i for service g. $\nu_{ji,g}$ is the sum of the proportion of new calls of service g accepted in cell j that go to cell i and the proportion of handoff calls with service g accepted from cells adjacent to cell j that go to cell i. Thus

$$\nu_{ji,g} = \lambda_{j,g}(1 - B_{j,g})q_{ji,g} + (1 - B_{j,g})q_{ji,g}\sum_{x\in\mathcal{A}_j} \nu_{xj,g}. \tag{5.6}$$

Equation (5.6) can be rewritten as

$$\nu_{ji,g} = \nu(B_{j,g}, \rho_{j,g}, q_{ji,g}) = (1 - B_{j,g})q_{ji,g}\rho_{j,g}, \tag{5.7}$$

where $\rho_{j,g}$, the total offered traffic to cell j for service g, is given by

$$\rho_{j,g} = \rho(\mathbf{v}, \lambda_{j,g}, \mathcal{A}_j) = \lambda_{j,g} + \sum_{x\in\mathcal{A}_j} \nu_{xj,g}, \tag{5.8}$$

and where $\mathbf{v}$ denotes the matrix whose components are the handoff rates ν_{ij} for $i, j = 1, ...M$.

The total offered traffic can be obtained from a fixed point model [32], which describes the offered traffic as a function of the handoff rates and new call arrival rates, the handoff rates as a function of the blocking probabilities and the offered traffic, and the blocking probabilities as a function of the offered traffic. For a given set of arrival rates, we use an iterative method to solve the fixed point equations. We define an initial value for the handoff rates. We calculate the offered traffic by adding the given values of the arrival rates to the handoff rates. The blocking probabilities are now calculated using the offered traffic. We then calculate the new values of the handoff rates and repeat. This approach has been extensively utilized in the literature to obtain solutions of fixed point problems [4, 37, 41, 66, 67, 68]. The questions of existence and uniqueness of the solution and whether the iterative approach in fact converges to the solution (if a unique solution exists) are generally difficult to answer due to the complexity of the equations involved. Kelly has shown that for fixed alternate routing the solution to the fixed point problem is in fact not unique [36]; in all the numerical examples we solved, the iterative approach converged to a unique solution.

5.4 WCDMA Call Admission Control

A CAC algorithm can be constructed as follows. A call arriving to cell i with service g is accepted if and only if the new state is a *feasible* state. Clearly this CAC algorithm requires global state, i.e., the number of calls in progress in all the cells of the network. Furthermore, to compute the blocking probabilities, the probability of each state in the feasible region needs to be calculated. Since the cardinality of Ω is $O({c_{eff}}^{M*G})$, the calculation of the blocking probabilities has a computational complexity that is exponential in the number of cells combined with number of available services.

In order to simplify the CAC algorithm, we consider only those CAC algorithms which utilize local state, i.e., the number of calls in progress in the current cell. To this end we

define a state $\mathbf{n}$ to be *admissible* if

$$n_{i,g} \leq N_{i,g} \quad \text{for} \quad i = 1, ..., M \text{ and } g = 1, ..., G, \tag{5.9}$$

where $N_{i,g}$ is a parameter which denotes the maximum number of calls with service g allowed to be admitted in cell i. Clearly the set of admissible states denoted Ω' is a subset of the set of feasible states Ω. The blocking probability for cell i with service g is then given by

$$B_{i,g} = B(A_{i,g}, N_{i,g}) = \frac{A_{i,g}^{N_{i,g}}/N_{i,g}!}{\sum_{k=0}^{N_{i,g}} A_{i,g}^{k}/k!}, \tag{5.10}$$

where $A_{i,g} = \rho_{i,g}/\mu_{i,g} = \rho_{i,g}/\mu(1 - q_{ii,g})$ is the Erlang traffic in cell i with service g. We note that the complexity to calculate the blocking probabilities in (5.10) is $O(M * G)$, and the bit error rate requirement is guaranteed since $\Omega' \subset \Omega$.

Once the maximum number of calls with different service that are allowed to be admitted in each cell, $\mathbf{N}$, is calculated (this is done offline and described in the next section), the CAC algorithm for cell i for service g will simply compare the number of calls with service g currently active in cell i to $N_{i,g}$ in order to accept or reject a new arriving call. Thus our CAC algorithm is implemented with a computational complexity that is $O(1)$.

5.5 Network Throughput

The throughput of cell i consists of two components: the new calls that are accepted in cell i minus the forced termination due to handoff failure of the handoff calls into cell i for all services g. Hence the total throughput, T, of the network is

$$T(\mathbf{B}, \rho, \lambda) = \sum_{i=1}^{M} \sum_{g=1}^{G} \left\{ \lambda_{i,g}(1 - B_{i,g}) - B_{i,g}(\rho_{i,g} - \lambda_{i,g}) \right\}, \tag{5.11}$$

where $\mathbf{B}$ is the vector of blocking probabilities and λ is the matrix of call arrival rates.

To study the effect of mobility and to differentiate between new calls and handoff calls, the throughput function can be generalized to a revenue function. The term *revenue* suggesting

an economic meaning is chosen to emphasize the rewards from not blocking a new call and the penalty (whether measured monetarily or by customer aggravation) from having handoff calls blocked. Hence the revenue, H, becomes

$$H(\mathbf{B}, \rho, \lambda) = \sum_{i=1}^{M} \sum_{g=1}^{G} \left\{ r_{i,g} \lambda_{i,g} (1 - B_{i,g}) - c_{i,g} B_{i,g} (\rho_{i,g} - \lambda_{i,g}) \right\}, \tag{5.12}$$

where $r_{i,g}$ is the revenue generated by accepting a new call with service g in cell i, and $c_{i,g}$ is the cost of a forced termination of a call with service g due to a handoff failure in cell i. The values of $r_{i,g}$ and $c_{i,g}$ control the tradeoff between new calls and handoff calls. The choice of $r_{i,g}$ and $c_{i,g}$ affect the CAC algorithm through their effect on $\mathbf{N}$. For example assume that $r_{i,g} = 1$ and $c_{i,g} = c_g$ for all i. Then, it is easy to see that for a given network topology the choice of larger c_g for service g will tend to increase the values of $\mathbf{N}$ for those cells into which the handoff rates are high while decreasing the values of $N_{i,g}$ for the other cells. These are tools that allow the system administrator to place more importance on handoff calls. Surveys and market studies investigating these issues help network administrators set these weights and achieve a desired tradeoff.

5.6 Calculation of $\mathbf{N}$

We formulate a constrained optimization problem in order to maximize the revenue subject to upper bounds on the blocking probabilities and a lower bound on the signal-to-interference constraints in (5.1). The goal is to optimize the utilization of network resources and provide consistent GoS while at the same time maintaining the QoS, β_g, for all the users for different services g. In this optimization problem the arrival rates are given and the maximum number of calls that can be admitted in all the cells are the independent variables. This is given in the following

$$
\begin{aligned}
\mathbf{N}=\begin{bmatrix} N_{1,1} & \dots & N_{1,G} \\ \dots & \dots & \dots \\ N_{M,1} & \dots & N_{M,G} \end{bmatrix} \quad & \max \quad H(\mathbf{B},\rho,\lambda), \\
\text{subject to} \quad & B(A_{i,g},N_{i,g}) \le \beta_g, \\
& \sum_{g=1}^{G} N_{i,g}v_g + \sum_{j=1,j\neq i}^{M}\sum_{g=1}^{G} N_{j,g}v_g\kappa_{ji,g} - v_g \le c_{eff}^{(g)}, \\
& \text{for} \quad i=1,\dots,M. \qquad (5.13)
\end{aligned}
$$

The optimization problem in (5.13) is solved offline to obtain the values of $\mathbf{N}$.

5.7 Maximization of Throughput

A second optimization problem can be formulated in which the arrival rates and the maximum number of calls that can be admitted in all the cells are the independent variables and the objective function is the throughput. This is given in the following

$$
\begin{aligned}
\max_{\lambda,\ \mathbf{N}} \quad & T(\mathbf{B},\rho,\lambda), \\
\text{subject to} \quad & B(A_{i,g},N_{i,g}) \le \beta_g, \\
& \sum_{g=1}^{G} N_{i,g}v_g + \sum_{j=1,j\neq i}^{M}\sum_{g=1}^{G} N_{j,g}v_g\kappa_{ji,g} - v_g \le c_{eff}^{(g)}, \\
& \text{for} \quad i=1,\dots,M. \qquad (5.14)
\end{aligned}
$$

The optimized objective function of (5.14) provides an upper bound on the total throughput that the network can carry. This is the *network capacity* for the given GoS and QoS.

5.8 Numerical Results

The following results have been obtained for a 27-cell CDMA network. The base stations are located at the centers of a hexagonal cell whose radius is 1732 m. Base station 1 is located at the center of the network; the base stations are numbered consecutively in a spiral pattern.

Table 5.1: The low mobility characteristics and parameters.

$\parallel \mathcal{A}_i \parallel$	$q_{ij,g}$	$q_{ii,g}$	$q_{i,g}$
3	0.020	0.240	0.700
4	0.015	0.240	0.700
5	0.012	0.240	0.700
6	0.010	0.240	0.700

The COST-231 propagation model [49] with a carrier frequency of 1800 MHz, average base station height of 30 m, and average mobile height of 1.5 m is used to determine the coverage region. The path-loss coefficient is 4. The shadow fading standard deviation is 6 dB and the processing gain is 6.02 dB, 12.04 dB, 18.06 dB, and 24.08 dB for Spreading Factor of 4, 16, 64, and 256, respectively. The bit-energy-to-interference ratio threshold is 7.5 dB with perfect power control for all four scenarios. The interference-to-background-noise ratio is 10 dB. The activity factor is 0.375.

Three mobility scenarios: no mobility, low mobility, and high mobility of users are considered. We assume that the mobility characteristics for a given service g stays the same throughout different cells in the network. The following parameters are used for the no mobility case: $q_{ij,g} = 0$, $q_{ii,g} = 0.3$ and $q_{i,g} = 0.7$ for all cells i and j. Tables 5.1 and 5.2 show respectively the mobility characteristics and parameters for the low and high mobility cases. In all three mobility scenarios, the probability that a call leaves the network after completing its dwell time is 0.7. Thus, regardless of where the call originates and mobility scenario used, the average dwell time of a call in the network is constant. In the numerical results below, for each SF value, we analyze the average throughput per cell by dividing the results from (5.14) by the total number of cells in the network and multiplying by the maximum data rate in Table 4.2.

Table 5.2: The high mobility characteristics and parameters.

$\parallel \mathcal{A}_i \parallel$	$q_{ij,g}$	$q_{ii,g}$	$q_{i,g}$
3	0.1	0	0.700
4	0.075	0	0.700
5	0.060	0	0.700
6	0.050	0	0.700

- $\parallel \mathcal{A}_i \parallel$ is the number of cells, which are adjacent to cell i.
- $q_{ii,g}$ is the probability that a call with service g in progress in cell i remains in cell i after completing its dwell time.
- $q_{ij,g}$ is the probability that a call with service g in progress in cell i after completing its dwell time goes to cell j.
- $q_{i,g}$ is the probability that a call with service g in progress in cell i departs from the network.

5.8.1 WCDMA Throughput Optimization with SF of 256

First, we set SF equal to 256, which is used to carry data for the control channel. Table 5.3 shows the optimized values of $\mathbf{N}$ for each cell for all three mobility models with perfect power control and 2% blocking probability. Fig. 5.1 shows the optimized throughput per cell for a blocking probability from 1% to 10%. The results for the average throughput for no mobility and high mobility cases are almost identical while the throughput for low mobility is higher for each blocking probability. The low mobility case has an equalizing effect on traffic resulting in slightly higher throughput.

5.8.2 WCDMA Throughput Optimization with SF of 64

Next, we set SF equal to 64, which is used for voice communication as shown in Fig. 4.3. As a result of lowering the SF to 64, the number of possible concurrent connections within one cell is also decreased. Because the throughput is calculated based on the number of simultaneous connections between MSs and BSs, the lower trunking efficiency [48] leads to

Table 5.3: Calculation of **N** for uniform user distribution with SF = 256 and blocking probability = 0.02.

	No Mobility	Low Mobility	High Mobility
Cell ID	N_i	N_i	N_i
$Cell_1$	52.86	52.86	52.86
$Cell_2$	53.95	53.95	53.95
$Cell_3$	51.84	51.84	51.84
$Cell_4$	51.84	51.84	51.84
$Cell_5$	53.95	53.95	53.95
$Cell_6$	51.85	51.85	51.85
$Cell_7$	51.85	51.85	51.85
$Cell_8$	53.00	53.00	53.00
$Cell_9$	50.73	50.73	50.73
$Cell_{10}$	62.74	62.74	62.74
$Cell_{11}$	63.29	63.29	63.29
$Cell_{12}$	62.73	62.73	62.73
$Cell_{13}$	50.73	50.73	50.73
$Cell_{14}$	53.01	53.01	53.01
$Cell_{15}$	50.73	50.73	50.73
$Cell_{16}$	62.71	62.71	62.71
$Cell_{17}$	63.27	63.27	63.27
$Cell_{18}$	62.71	62.71	62.71
$Cell_{19}$	50.74	50.74	50.74
$Cell_{20}$	73.40	73.40	73.40
$Cell_{21}$	71.84	71.84	71.84
$Cell_{22}$	71.86	71.86	71.86
$Cell_{23}$	73.43	73.43	73.43
$Cell_{24}$	73.43	73.43	73.43
$Cell_{25}$	71.83	71.83	71.83
$Cell_{26}$	71.82	71.82	71.82
$Cell_{27}$	73.40	73.40	73.40

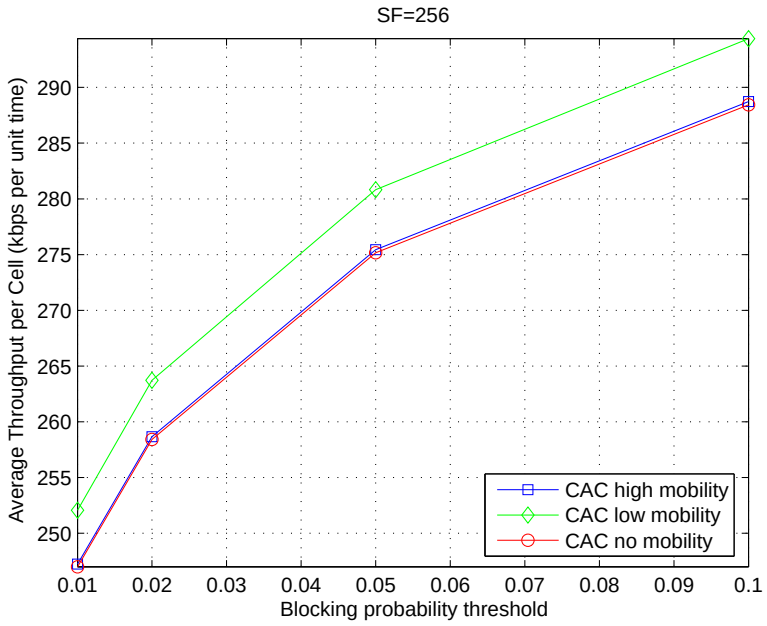

Figure 5.1: Average throughput in each cell for SF = 256.

lower throughput as shown in Fig. 5.2. Table 5.4 shows the optimized values of **N** for each cell for all three mobility cases and SF equal to 64.

5.8.3 WCDMA Throughput Optimization with SF of 16

Next, we set SF equal to 16, which is used for 64 Kbps data communication as shown in Fig. 4.4. As a result of lowering the SF to 16, the average number of slots within one cell decreases to 4.30 as was shown in Table 4.5. The resulting throughput, as shown in Fig. 5.3, is much lower compared to the case with SF equal to 64 or 256. Table 5.5 shows the optimized values of **N** for each cell for all three mobility cases with SF equal to 16.

5.8.4 WCDMA Throughput Optimization with SF of 4

Next, we set SF equal to 4, which is normally used for 256 Kbps data communication between BSs and MSs. As a result of lowering the SF to 4, the average slots per sector decreases significantly to 1.49 with perfect power control and $\frac{E_b}{I_0} = 7.5$ dB as shown in Fig. 4.8. Table

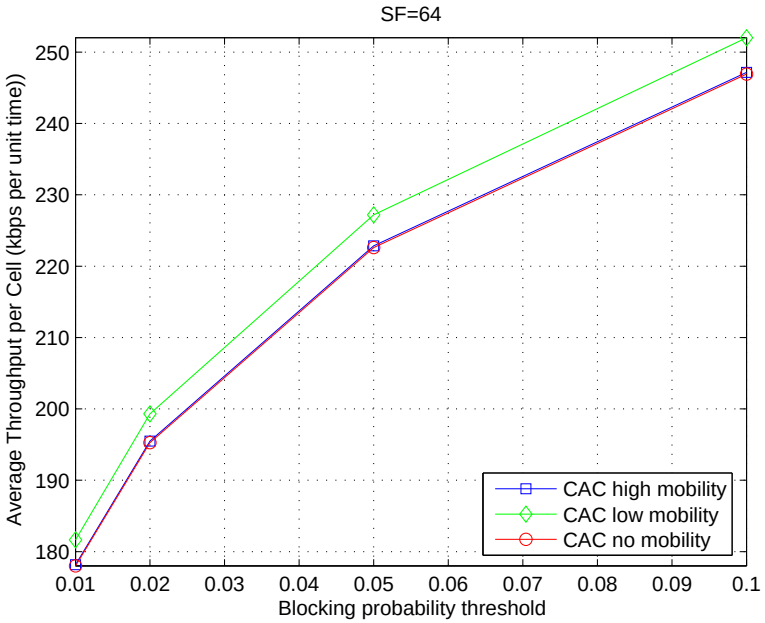

Figure 5.2: Average throughput in each cell for SF = 64.

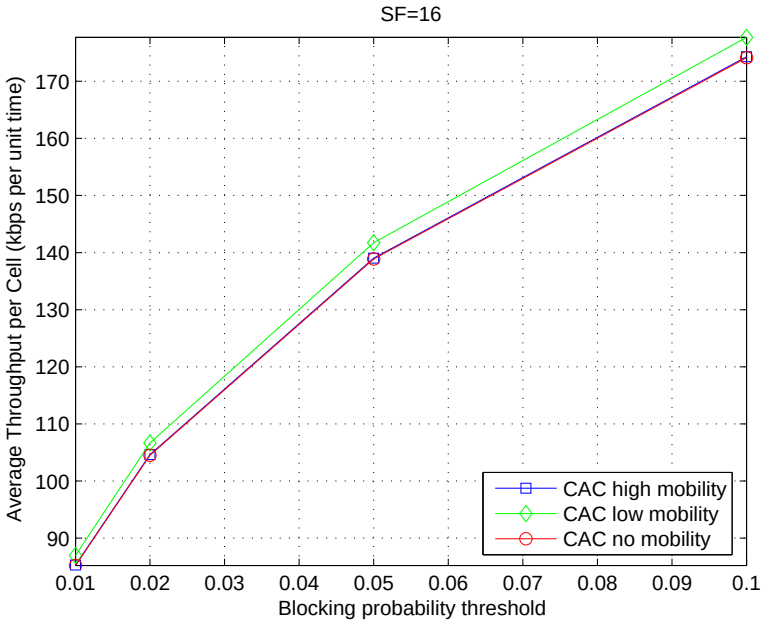

Figure 5.3: Average throughput in each cell for SF = 16.

Table 5.4: Calculation of **N** for uniform user distribution with SF = 64 and blocking probability = 0.02.

	No Mobility	Low Mobility	High Mobility
Cell ID	N_i	N_i	N_i
$Cell_1$	13.58	13.58	13.58
$Cell_2$	13.86	13.86	13.86
$Cell_3$	13.32	13.32	13.32
$Cell_4$	13.32	13.32	13.32
$Cell_5$	13.86	13.86	13.86
$Cell_6$	13.32	13.32	13.32
$Cell_7$	13.32	13.32	13.32
$Cell_8$	13.61	13.61	13.61
$Cell_9$	13.03	13.03	13.03
$Cell_{10}$	16.11	16.11	16.11
$Cell_{11}$	16.26	16.26	16.26
$Cell_{12}$	16.11	16.11	16.11
$Cell_{13}$	13.03	13.03	13.03
$Cell_{14}$	13.62	13.62	13.62
$Cell_{15}$	13.03	13.03	13.03
$Cell_{16}$	16.11	16.11	16.11
$Cell_{17}$	16.25	16.25	16.25
$Cell_{18}$	16.11	16.11	16.11
$Cell_{19}$	13.03	13.03	13.03
$Cell_{20}$	18.85	18.85	18.85
$Cell_{21}$	18.45	18.45	18.45
$Cell_{22}$	18.46	18.46	18.46
$Cell_{23}$	18.86	18.86	18.86
$Cell_{24}$	18.86	18.86	18.86
$Cell_{25}$	18.45	18.45	18.45
$Cell_{26}$	18.45	18.45	18.45
$Cell_{27}$	18.85	18.85	18.85

Table 5.5: Calculation of **N** for uniform user distribution with SF = 16 and blocking probability = 0.02.

	No Mobility	Low Mobility	High Mobility
Cell ID	N_i	N_i	N_i
$Cell_1$	3.75	3.75	3.75
$Cell_2$	3.83	3.83	3.83
$Cell_3$	3.68	3.68	3.68
$Cell_4$	3.68	3.68	3.68
$Cell_5$	3.83	3.83	3.83
$Cell_6$	3.68	3.68	3.68
$Cell_7$	3.68	3.68	3.68
$Cell_8$	3.76	3.76	3.76
$Cell_9$	3.60	3.60	3.60
$Cell_{10}$	4.46	4.46	4.46
$Cell_{11}$	4.50	4.50	4.50
$Cell_{12}$	4.46	4.46	4.46
$Cell_{13}$	3.60	3.60	3.60
$Cell_{14}$	3.77	3.77	3.77
$Cell_{15}$	3.60	3.60	3.60
$Cell_{16}$	4.45	4.45	4.45
$Cell_{17}$	4.49	4.49	4.49
$Cell_{18}$	4.45	4.45	4.45
$Cell_{19}$	3.60	3.60	3.60
$Cell_{20}$	5.21	5.21	5.21
$Cell_{21}$	5.10	5.10	5.10
$Cell_{22}$	5.10	5.10	5.10
$Cell_{23}$	5.22	5.22	5.22
$Cell_{24}$	5.22	5.22	5.22
$Cell_{25}$	5.10	5.10	5.10
$Cell_{26}$	5.10	5.10	5.10
$Cell_{27}$	5.21	5.21	5.21

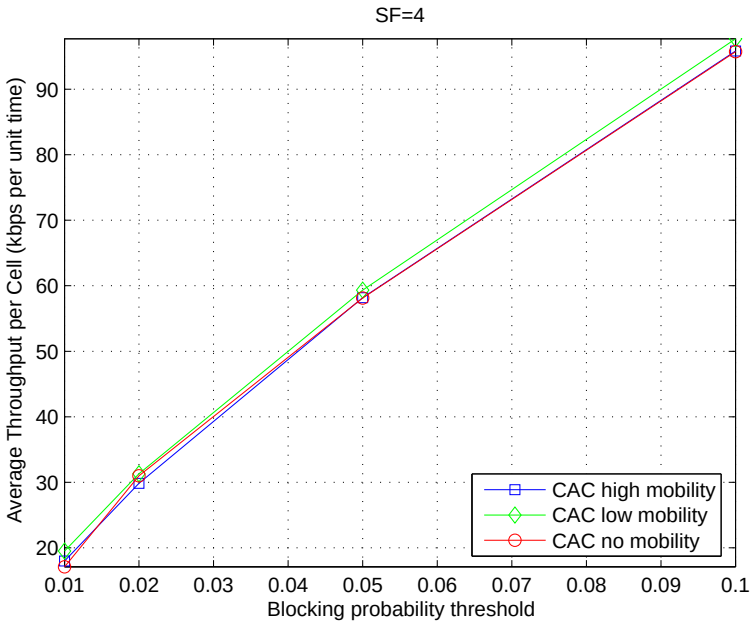

Figure 5.4: Average throughput in each cell for SF = 4.

5.5 shows the optimized values of **N** for each cell for all three mobility models with SF equal to 4. The average throughput for all three mobility cases are almost identical as shown in Fig. 5.4.

5.9 Conclusions

An analytical model has been presented for CAC algorithm for optimizing the throughput in multi-cell WCDMA networks. For the high mobility case, every connection moves to a new cell, which is equivalent to having new calls in every cell for each dwell time. Thus, the throughput for the no mobility and high mobility scenarios are identical. However, the throughput for the low mobility scenario is slightly higher because of the equalizing effect on traffic due to low mobility. Numerical results show that as the spreading factor increases, the optimized throughput is better, due to the trunking efficiency for all the three mobility models. Our CAC algorithm is computationally efficient and can be implemented for large multi-cell WCDMA networks.

Table 5.6: Calculation of **N** for uniform user distribution with SF = 4 and blocking probability = 0.02.

	No Mobility	Low Mobility	High Mobility
Cell ID	N_i	N_i	N_i
$Cell_1$	1.24	1.16	1.32
$Cell_2$	1.48	1.42	1.24
$Cell_3$	1.30	1.32	1.28
$Cell_4$	1.30	1.32	1.28
$Cell_5$	1.48	1.42	1.23
$Cell_6$	1.30	1.32	1.28
$Cell_7$	1.30	1.32	1.28
$Cell_8$	0.94	1.37	1.23
$Cell_9$	0.93	0.94	1.27
$Cell_{10}$	1.59	1.58	1.54
$Cell_{11}$	1.53	1.53	1.55
$Cell_{12}$	1.59	1.58	1.54
$Cell_{13}$	0.93	0.94	1.27
$Cell_{14}$	0.94	1.37	1.23
$Cell_{15}$	0.93	0.93	1.27
$Cell_{16}$	1.59	1.58	1.54
$Cell_{17}$	1.53	1.53	1.55
$Cell_{18}$	1.59	1.58	1.54
$Cell_{19}$	0.93	0.93	1.27
$Cell_{20}$	1.92	1.83	1.82
$Cell_{21}$	1.79	1.80	1.76
$Cell_{22}$	1.79	1.80	1.76
$Cell_{23}$	1.92	1.83	1.82
$Cell_{24}$	1.92	1.83	1.82
$Cell_{25}$	1.79	1.80	1.76
$Cell_{26}$	1.79	1.80	1.76
$Cell_{27}$	1.92	1.83	1.82

CHAPTER 6

CONCLUSIONS

6.1 Summary

Compared to other multiple access technologies like FDMA and TDMA, which divide the total bandwidth to frequency sub-bands and time slots, respectively, CDMA is an unique multiple access technology, where all users share the entire available bandwidth to transmit and receive information. Interference generated by users in the network is the main limitation for determining the network capacity. A large number of researchers in CDMA use average interference for designing call admission control and calculating capacity. The advantage gained from this method over actual interference is a huge reduction in computational complexity.

In Chapter 2, we provided an overview of CDMA and WCDMA. This chapter summarized the features, which demonstrated CDMA's superiority over other 2G cellular networks. In addition, this chapter also introduced the requirements for 3G cellular systems, which included wider bandwidth allocations, as well as new additional features.

User modeling enables the computation of the traffic density in the cellular network, which can be used to optimize the placement of BSs and radio network controllers as well as to analyze the performance of resource management algorithms towards meeting the final goal: the calculation and maximization of network capacity. In Chapter 3, we presented an analytical model for approximating the user distributions in multi-cell WCDMA networks using a 2-dimensional Gaussian function by determining the means and the standard deviations of the distributions for every cell. This allowed for the calculation of the intra-cell and inter-cell interference, and the reverse-link capacity of the network. We analyzed three

scenarios of user distribution using 2-D Gaussian function: uniform distribution of users, users densely clustered at the center of the cells, and users distributed at cells' boundaries.

In Chapter 4, we maximized the capacity in multi-cell WCDMA networks. Optimizing capacity was calculated with different spreading factors of 256, 64, 16, and 4. Numerical results showed that the SIR threshold for the received signals was decreased by 0.5 to 1.5 dB due to the imperfect power control. As expected, we can have many low rate voice users or fewer data users as the data rate increases. The results also showed that the determined parameters of the 2-dimensional Gaussian model matched well with the traditional method for modeling user distribution.

In Chapter 5, we designed a call admission control algorithm for optimizing the throughput in multi-cell WCDMA networks. Numerical results were analyzed for no, low, and high mobility scenarios. The results showed that as the spreading factor increases, due to trunking efficiency, the optimized throughput is better for all the three mobility cases. Our method of optimizing capacity and throughput is computationally efficient and can be implemented for large multi-cell WCDMA networks.

6.2 Future Research

We conclude by outlining possible directions for future research:

As shown in Table 4.2, the maximum transfer data rate is only 480 Kbps when used with a spreading factor of 4 in the 5 MHz spectrum. To achieve the promised speed of 2 Mbps data rate in 3G systems, 6 parallel codes with a spreading factor of 4 need to be used. Further research can delve into how to use and interact between these parallel codes, and how the interference level is generated and capacity is calculated in each cell in WCDMA networks with 2x60 MHz spectrum (1710-1770 MHz and 2110-2170 MHz). The new IMT-2000 spectrum of 190 MHz (2500-2690 MHz) arrangement is still under development.

BIBLIOGRAPHY

[1] 3GPP. 3GPP specifications - releases, phases, and stages. http://www.3gpp.org/specs/releases.htm.

[2] R.G. Akl, M. Hegde, and M. Naraghi-Pour. Mobility-based CAC algorithm for arbitrary traffic distribution in CDMA cellular systems. *IEEE Trans. Veh. Technol.*, 54:639–651, March 2005.

[3] R.G. Akl, M.V. Hegde, A. Chandra, and P.S. Min. CCAP: CDMA Capacity Allocation and Planning. Technical report, Washington University, April 1998.

[4] R.G. Akl, M.V. Hegde, and P.S. Min. Effects of call arrival rate and mobility on network throughput in multi-cell CDMA. *IEEE International Conf. on Commun.*, 3:1763–1767, June 1999.

[5] R.G. Akl, M.V. Hegde, M. Naraghi-Pour, and P.S. Min. Multi-cell CDMA network design. *IEEE Trans. Veh. Technol.*, 50(3):711–722, May 2001.

[6] R.G. Akl and A. Parvez. Impact of interference model on capacity in CDMA cellular networks. *Proceedings of SCI 04: Communication and Network Systems, Technologies and Applications*, 3:404–408, July 2004.

[7] S. Anand, A. Chockalingam, and K. N. Sivarajan. Outage and capacity analysis of cellular CDMA with admission control. *IEEE Wireless Commun. and Networking Conf.*, 2:908–912, March 2002.

[8] S. Ariyavisitakul and L.F. Chang. Signal and interference statistics of a CDMA system with feedback power control. *Global Telecommunications Conf.*, 2:1490–1495, December 1991.

[9] M. Asawa and W.E. Stark. Optimal scheduling of soft handoffs in DS/CDMA communication systems. *Fourteenth Annual Joint Conf. of the IEEE Computer and Commun. Societies*, 1:105 – 112, April 1995.

[10] A. Baiocchi, F. Sestini, and F. Priscoli. Effects of user mobility on the capacity of a CDMA network. *European Trans. on Telecommunications*, 7(4):305–314, July-August 1996.

[11] P. Balaban and J. Salz. Optimum diversity combining and equalization in digital data transmission with applications to cellular mobile radio I. Theoretical considerations. *IEEE Trans. Commun.*, 40:885–894, May 1992.

[12] P. Balaban and J. Salz. Optimum diversity combining and equalization in digital data transmission with applications to cellular mobile radio II. Numerical results. *IEEE Trans. Commun.*, 40:895–907, May 1992.

[13] Mary Bellis. Selling the cell phones - history of cellular phones. http://inventors.about.com/library/weekly/aa070899.htm.

[14] J.O. Carnero, K.I. Pedersen, and P.E. Mogensen. Capacity gain of an uplink-synchronous WCDMA system under channelization code constraints. *IEEE Veh. Technol. Conf.*, 53:982 – 991, July 2004.

[15] CDMA Development Group. CDG : Worldwide : 4Q 2004 CDMA Subscribers Statistics. http://www.cdg.org/worldwide/cdma_world_subscriber.asp.

[16] CDMA Development Group. CDG : Worldwide : CDMA Worldwide. http://www.cdg.org/worldwide/index.asp?h_area=0.

[17] M. Chopra, K. Rohani, and J.D. Reed. Analysis of CDMA range extension due to soft handoff. *IEEE Veh. Technol. Conf.*, 2:917 – 921, July 1995.

[18] G. Cimone, D.D. Weerakoon, and A.H. Aghvami. Performance evaluation of a two layer hierarchical cellular system with variable mobility users using multiple class applications. *IEEE Veh. Technol. Conf.*, 5:2835–2839, September 1999.

[19] T. Dohi, M. Sawahashi, and F. Adachi. Performance of SIR based power control in the presence of non-uniform traffic distribution. *IEEE International Conf. on Universal Personal Commun.*, pages 334–338, November 1995.

[20] J.S. Evans and D. Everitt. On the teletraffic capacity of CDMA cellular networks. *IEEE Trans. Veh. Technol.*, 48(1):153–165, January 1999.

[21] Adachi F., Sawahashi M., and Okawa K. Tree-structured generation of orthogonal spreading codes with different lengths for forward link of DS-CDMA mobile radio. *Electr. Lett.*, 33:27–28, January 1997.

[22] E.D. Fitkov-Norris and A. Khanifar. Dynamic pricing in cellular networks, a mobility model with a provider-oriented approach. *3G Mobile Commun. Technol.*, pages 63 – 67, March 2001.

[23] G.J. Foschini and Z. Miljanic. A simple distributed autonomous power control algorithm and its convergence. *IEEE Trans. Veh. Technol.*, 42(4):641–646, November 1993.

[24] H. Fu and J.S. Thompson. Downlink capacity analysis in 3GPP WCDMA networks system. *3G Mobile Commun. Technol.*, pages 534–538, May 2002.

[25] V.K. Garg. *IS-95 CDMA and CDMA2000: Cellular/PCS Systems Implementation.* Prentice Hall communications engineering and emerging technologies series, 2000.

[26] K.S. Gilhousen, I.M. Jacobs, R. Padovani, A.J. Viterbi, L.A. Weaver, and C.E. Wheatley. On the capacity of a cellular CDMA system. *IEEE Trans. Veh. Technol.*, 40(2):303–312, May 1991.

[27] S.V. Hanly. Capacity and power control in spread spectrum macrodiversity radio networks. *IEEE Trans. Commun.*, 44(2):247–256, February 1996.

[28] S.V. Hanly. An algorithm for combined cell-site selection and power control to maximize cellular spread spectrum capacity. *IEEE J. Select. Areas Commun.*, 13(7):1332–1340, September 1995.

[29] H. Holma and A. Toskala. *WCDMA for UMTS: Radio Access for Third Generation Mobile Communication.* John Wiley & Sons, Ltd., 2002.

[30] infoSync World. infoSync World : 1.87 billion mobile users by 2007. http://www.infosyncworld.com/news/n/5048.html.

[31] Y. Ishikawa and N. Umeda. Capacity design and performance of call admission control in cellular CDMA systems. *IEEE J. Select. Areas Commun.*, 15(8):1627–1635, October 1997.

[32] V.I. Istratescu. *Fixed Point Theory : An Introduction.* D. Reidel, 1981.

[33] S.H. Jeong and J.A. Copeland. Cell loss ratio and multiplexing gain of an ATM multiplexer for VBR voice sources. *Local Computer Networks*, pages 384–389, Oct 1998.

[34] Dan Jones. Air interfaces - what are they? http://www.unstrung.com/document.asp?doc_id=15195&page_number=9.

[35] V.M. Jovanovic and D. Cuberovic. Theoretical and experimental analysis of the new soft handoff algorithm for CDMA systems. *IEEE Veh. Technol. Conf.*, 3:1757 – 1762, May 2000.

[36] F.P. Kelly. Blocking probabilities in large circuit switched networks. *Advances in Applied Probability*, 18:473–505, 1986.

[37] F.P. Kelly. Routing in circuit-switched network: Optimization, shadow prices and decentralization. *Advances in Applied Probability*, 20:112–144, 1988.

[38] Kyoung II Kim. CDMA cellular engineering issues. *IEEE Veh. Technol. Conf.*, 42:345–350, August 1993.

[39] Z. Liu, Y. Wang, and D. Yang. Effect of soft handoff parameters and traffic loads on soft handoff ratio in CDMA systems. *International Conf. on Communication Technology Proceedings*, 2:782 – 785, April 2003.

[40] David W. Matolak and Anjula Thakur. Outside cell interference dynamics in cellular CDMA. *Proceedings of the 35th Southeastern Symposium*, pages 418–152, March 2003.

[41] D. Mitra, J.A. Morrison, and K.G Ramakrishnan. ATM network design and optimization: a multirate loss network framework. *IEEE/ACM Trans. on Networking*, 4(4):531–543, August 1996.

[42] A.F. Naguib, A. Paulraj, and T. Kailath. Capacity improvement of base-station antenna arrays cellular CDMA. *Conf. Record of The Twenty-Seventh Asilomar Conf. on Signals, Systems and Computers*, 2:1437–1441, November 1993.

[43] S. Nguyen and R. Akl. Approximating user distributions in WCDMA networks using 2-D Gaussian. *International Conf. on Comput., Commun., and Control Technol.*, July 2005, accepted.

[44] S. Nousiainen, K. Kordybach, and P. Kemppi. User distribution and mobility model framework for cellular network simulations. *IST Mobile & Wireless Telecommunications Summit*, pages 518–522, June 2002.

[45] T. Ojanpera, J. Skold, J. Castro, L. Girard, and A. Klein. Comparison of multiple access schemes for UMTS. *IEEE Veh. Technol. Conf.*, 2:490–494, May 1997.

[46] R. Padovani. Reverse link performance of IS-95 based cellular systems. *IEEE Personal Commun. Mag.*, 1(3):28–34, Third Quarter 1994.

[47] Bruce M. Penrod. A new class of precision UTC and frequency reference using IS-95 CDMA base station transmissions. http://www.endruntechnologies.com/pdf/PTTI2001_WhitePaper.pdf.

[48] Theodore S. Rappaport. *Wireless Communications: Principles and Practice*. Prentice Hall, 2001.

[49] T.S. Rappaport. *Wireless Communications Principles and Practice*. Prentice Hall, 1996.

[50] K.V. Ravi. Comparison of multiple-accessing schemes for mobile communication systems. *IEEE International Conf. on Personal Wireless Commun.*, pages 152–156, August 1994.

[51] C.U. Saraydar and A. Yener. Capacity enhancement for CDMA systems through adaptive cell sectorization. *IEEE Wireless Commun. and Networking Conf.*, pages 1139–1143, September 1999.

[52] S. Seo, T. Dohi, and F. Adachi. SIR-Based transmit power control of reverse link for coherent DS-CDMA mobile radio. *IEICE Trans. on Commun.*, E81-B(7):1508–1516, July 1998.

[53] S. Shin, C. Cho, and D. Sung. Interference-based channel assignment for DS-CDMA cellular systems. *IEEE Trans. Veh. Technol.*, 48(1):233–239, January 1999.

[54] Y.M. Siu and K.K. Soo. CDMA mobile systems with tailor made power control to each mobile station. *3G Mobile Commun. Technol.*, pages 46–50, March 2000.

[55] D. Staehle, K. Leibnitz, K. Heck, B. Schroder, A. Weller, and P. Tran-Gia. Approximating the othercell interference distribution in inhomogenous UMTS networks. *IEEE Veh. Technol. Conf.*, 4:1640–1644, May 2002.

[56] B. Suard, A.F. Naguib, G. Xu, and A. Paulraj. Performance of CDMA mobile communication systems using antenna arrays. *IEEE International Conf. on Acoustics, Speech, and Signal Processing*, 4:153 – 166, April 1993.

[57] S.C. Swales, M.A. Beach, D.J. Edwards, and J.P. McGeehan. The performance enhancement of multibeam adaptive base-station antennas for cellular land mobile radio systems. *IEEE Trans. Veh. Technol.*, 39:56 – 67, February 1990.

[58] K. Tachikawa. *W-CDMA: Mobile Communications System.* John Wiley & Sons, Ltd., 2002.

[59] K. Takeo and S. Sato. Evaluation of a CDMA cell design algorithm considering nonuniformity of traffic and base station locations. *IEICE Trans. Fundamentals*, E81-A(7):1367–1377, July 1998.

[60] K. Takeo and S. Sato. The proposal of CDMA cell design scheme considering change in traffic distributions. *IEEE International Symposium on Spread Spectrum Techniques and Applications*, 1:229–233, September 1998.

[61] Y. Takeuchi. Results of multiple cell simulations of a CDMA cellular system focusing on SIR based power control. *IEEE International Conf. on Commun.*, 1:63–67, June 1998.

[62] C. Tellez-Labao, J.M. Romero-Jerez, and A. Diaz-Estrella. Capacity analysis of SIR-based power-controlled CDMA systems under multipath fading. *IEEE International Symposium on Personal, Indoor, and Mobile Radio Commun.*, 3:1237–1241, September 2002.

[63] TIA/EIA. Mobile station-base station compatibility standard for wideband spread spectrum cellular systems. Technical report, IS-95B, March 1999.

[64] TIA/EIA. Mobile station-base station compatibility standard for dual-mode wideband spread spectrum cellular system. Technical report, IS-95A, May 1995.

[65] C. Vargas, M. Hegde, and M. Naraghi-Pour. Implied costs for multi-rate wireless networks. *J.Wireless Networks*, 10:323 337, May 2004.

[66] C. Vargas, M.V. Hegde, and M. Naraghi-Pour. Blocking effects of mobility and reservations in wireless networks. *IEEE International Conf. on Commun.*, 3:1612–1616, June 1998.

[67] C. Vargas, M.V. Hegde, and M. Naraghi-Pour. Implied costs in wireless networks. *IEEE Veh. Technol. Conf.*, 2:904–908, May 1998.

[68] C. Vargas-Rosales. *Communication Network Design and Evaluation Using Shadow Prices*. PhD thesis, Louisiana State University, 1996.

[69] A.J. Viterbi. *CDMA Principles of Spread Spectrum Communication*. Addison-Wesley, 1995.

[70] A.J. Viterbi, A.M. Viterbi, K.S. Gilhousen, and E. Zehavi. Soft handoff extends CDMA cell coverage and increases reverse link capacity. *IEEE J. Select. Areas Commun.*, 12:1281–1288, October 1994.

[71] A.J. Viterbi, A.M. Viterbi, K.S. Gilhousen, and E. Zehavi. Soft handoff extends CDMA cell coverage and increases reverse link capacity. *IEEE J. Select. Areas Commun.*, 12(8):1281–1288, October 1994.

[72] A.M. Viterbi and A.J.Viterbi. Erlang capacity of a power controlled CDMA system. *IEEE J. Select. Areas Commun.*, 11(6):892–900, August 1993.

[73] J.H. Wen, J.S. Sheu, and J.L. Chen. An optimum downlink power control method for CDMA cellular mobile systems. *IEEE International Conf. on Commun.*, 6:1738–1742, June 2001.

[74] D. Wong and T. J. Lim. Soft handoffs in CDMA mobile systems. *IEEE Personal Commun. Mag.*, 4:6–17, December 1997.

[75] B. Worley and F. Takawira. Handoff schemes in CDMA cellular systems. *Proceedings of Commun. and Signal Processing 1998*, pages 255 – 260, Sept. 1998.

[76] Q. Wu. Performance of optimum transmitter power control in cellular radio systems. *IEEE Trans. Veh. Technol.*, 48:571–575, March 1999.

[77] R.D. Yates. A framework for uplink power control in cellular radio systems. *IEEE J. Select. Areas Commun.*, 13(7):1341–1347, September 1995.

[78] Q. Zhang. UMTS air interface voice/data capacity-part 2: forward link analysis. *IEEE Veh. Technol. Conf.*, 4:2730 – 2734, May 2001.

[79] Q. Zhang and O. Yue. UMTS air interface voice/data capacity-part 1: reverse link analysis. *IEEE Veh. Technol. Conf.*, 4:2725 – 2729, May 2001.